Flood Modelling in Perfume River Basin, Hue Province, Vietnam

Piero Villegas
March, 2004

Flood Modelling in Perfume River Basin, Hue Province, Vietnam

by

Piero Villegas

Thesis submitted to the International Institute for Geo-information Science and Earth Observation in partial fulfilment of the requirements for the degree of Master of Science in Water Resources and Environmental Management.

Degree Assessment Board

Prof. A. M. J. Meijerink (Chairman)
WRES Division, ITC
Dr. L. M. Bouwer (External Examiner)
Free University Amsterdam
A. Gieske (Supervisor)
WRES Division, ITC
A. M. van Lieshout (Member, Second Supervisor)
WRES Division, ITC

INTERNATIONAL INSTITUTE FOR GEO-INFORMATION SCIENCE AND EARTH OBSERVATION
ENSCHEDE, THE NETHERLANDS

Disclaimer

This document describes work undertaken as part of a programme of study at the International Institute for Geo-information Science and Earth Observation. All views and opinions expressed therein remain the sole responsibility of the author, and do not necessarily represent those of the institute. Data used in the thesis will not be used for publishing without written permission of the thesis supervisor

Dedicated to my Parents

Acknowledgements

I wish to express my appreciation to the Government of the Netherlands for granting me with a scholarship to pursue a course in the ITC, through the Netherlands Fellowship Program. My sincere and special thanks to my supervisor Ambro Gieske for his valuable guidance, advices and constructive criticism through this research. I would like to extend my sincere thanks to Dr. Tjeerd Hobma for his suggestions of the thesis topic, encouragement at the beginning of the research and for giving me the opportunity to make a fieldwork in Vietnam. Many thanks also to Laurens Bouwer and Jeroen Aerts for their advices and help during my visits to the Free University.

My gratitude to the persons in Vietnam that provided us with the data that was used in this research, especially to Robbert Misdorp, Mr. Tran Dinh Lan from the Haiphong Institute of Oceanography, Nguyen Dinh Duong from the Institute of Geography and Levan Thu from the VN-ICZM project for provide us with the data used in this study. Many thanks also to Jeanette Mulder from Tropenbos International in Vietnam.

Many thanks to my friends in the ITC to give me the friendship and support that I will never forget.

Abstract

During recent years several large floods have caused disasters in Southeast Asia. The inundation and flooding in the central region of Vietnam are a serious problem. The combination of an extended flat territory in the long coastline and the frequent tropical storms makes this a recurrent problem. The hydro-meteorological network system, although was equipped with the full necessary instruments, they are still ordinary, with very low level of modernization and it is sparse

In the last years rainfall estimation based on remote sensors has been carried out on board of several launched platforms. One of these is the Tropical Rainfall Measuring Mission (TRMM). This satellite collects data of rainfall around the tropical regions of the planet. In the present study, data of this sensor was compared with ground rain gauge records through the discharges obtained by GIS modeling. STREAM (Spatial Tools for River basins and Environment and Analysis of Management options) is a GIS raster model that simulates discharges in a river basin using a spatial water balance model. For this study the model, originally based in monthly steps, was changed to daily to model the flood event. The comparison between the results with rainfall data collected in the ground and the TRMM rainfall shows that the most reliable estimation during the flooding period so far is the TRMM data. Nevertheless, the rain gauge collected data is more efficient during the normal conditions.

With the actual flooding area extracted from three RADARSAT images, a Reservoir model was developed to estimate the Volume of water stored in the flood plain, and the output according to the inputs obtained. The use of a DEM inundation technique was useful to find the relationship between volume and water level and, in this way, the temporal variation of the flood was estimated. With this model a Residence Time into the flood plain of 2.1 days was found.

TABLE OF CONTENTS

LIST OF FIGURES

LIST OF TABLES

LIST OF ABREVATIONS

AVHRR:	Advanced Very High Resolution Radiometer
CCP:	Coastal Cooperative Program
CZMC:	Coastal Zone Management Centre, The Hague
DAAC:	Distributed Active Archive Center
GES:	Goddard Earth Sciences
GOES:	Geoestationary Satellite
HMS:	Hydrometeorological Service of Vietnam
IR:	Infrared spectrum
IVM:	Institute of Environmental Studies
METEOSAT:	Meteorological Satellite
MW:	Microwave spectrum
NASA:	National Aeronautics and Space Administration
NOAA:	National Oceanic and Atmospheric Administration
NPMOC / JTWC:	Naval Pacific Meteorology and Oceanography Center / Joint Typhoon Warning Center
RIKZ:	Rijksinstituut voor Kust en Zee
SAR:	Synthetic Aperture Radar
STREAM	Spatial Tools for River basins and Environment and Analysis of Management options
TCFA:	Tropical Cyclone Forecast Alert
TRMM:	Tropical Rainfall Measuring Mission
VIS:	Visible spectrum
VN-ICZM:	Vietnamese Netherlands Integrated Coastal Zone Management

1. Introduction

1.1. Background

Understanding the climate and how to respond to climate perturbations relies on what we know about the many factors that interact in the atmosphere. These factors are atmospheric moisture, clouds, latent heat winds, pressure and precipitation. The physical process that links these key elements is precipitation, which directly affects the generation of clouds and large-scale motions and thus indirectly influences the distribution of moisture and the greenhouse warming in the earth's atmosphere. The present day's knowledge in rainfall distribution is limited, especially over the oceans and the tropics. Spaceborne rainfall sensors are needed to understand the water cycles in our planet. There would be also useful to integrate databases collected in rainfall stations in a well spatial distributed way and obtain data where there is lack of collected rainfall data. This problem is really pronounced in the Tropics where the conventional observation network is sparse and rainfall analyses are typically based largely on model-generated estimates sensitive to the physical parameterization scheme employed in the assimilation system. On the other hand, the observation-based rainfall estimates suffer from uncertainties in retrieval algorithms and inadequate sampling, and can provide but an estimation of the truth (Hou, Zhang et al. 2001)

In the case of Vietnam, in the last years the hydro-meteorological network system was equipped with the full necessary instruments. However, these observation instruments are still ordinary, with very low level of modernization and automization. The data collection, processing, transmitting/receiving are mainly done manually. The collected data are processed manually using tables, monographs and graphics and the data checking is mainly based on the experience of local experts. For this reason another source of rainfall data is needed and more in the case of this region were rainfall rates are high and are accompanied by frequent flooding.

In the last years rainfall estimation based on remote sensors in the visible (VIS), infrared (IR) radar, and microwave (MW) ranges of the spectrum, has been carried out on board of several launched platforms. In particular, the launch of the newest generation of geostationary satellites, the Geostationary Operational Environmental Satellite GOES-I-M series (Menzel and Purdom 1994) and the newest METEOSAT Second Generation (MSG) (Schmetz, Pili et al. 2002) with its Spinning Enhanced Visible and Infrared Imager (SEVIRI), adds new channels to the traditional VIS-IR-WV (Water Vapor) triplet. Some of the new channels have been tested for decades as part of the Advanced Very High Resolution Radiometer (AVHRR) series on board the National Oceanic and Atmospheric Administration (NOAA) polar orbiters or have other heritages (Levizzani and Amorati 2002).

One of the spaceborne rainfall sensors that nowadays is becoming an object of interest by the scientific community is the Tropical Rainfall Measure Mission (TRMM) that is based in algorithms to estimate the 3D rain distribution from visual spectrum radiances, radar and microwave sensors. This

sensor has been applied in several cases that include storms and typhoons monitoring (Rui, Teng et al. 2002).

During recent years several large floods have caused disasters in Southeast Asia. Historically there have always been floods, but the frequency of serious ones during the last few years has increased policy attention regarding disaster mitigation. The inundation and flooding in the central region of Vietnam are a serious problem of the whole country. The combination of an extended flat territory in the long coastline and the frequent tropical storms makes of this a recurrent problem.

In November 1999 disaster floods struck eight provinces in central Vietnam, particularly in Thua Thien Hue and Quang Nam provinces. 2700 mm of rain fell in four days and caused serious damage to livelihood and production systems in both upland and lowland areas. Seven hundred people died in the region. There was land erosion, land inundation with sand and stones, destruction of growing crops due to waterlogged root systems, loss of animals, loss of crops in storage, damage to houses, damage to water management infrastructure, roads and bridges etc. The floods in the mountain and hilly areas were mainly characterized by flash floods, with the destruction caused by the power of the massive water flow. In more low-lying areas the main damage was caused by the long inundation with high water levels, reaching up to two meters in the houses for several days.

In the past years, the methods of research and establishment of maps on inundation caused by rise of the sea level in the coastal area or flooding level were implemented by many organizations in Vietnam. These studies have been carried out to establish damage maps in the most of the cases. The goal of the inundation mapping is to facilitate the authorities at all levels and the people of the Central provinces to limit the damages due to the floods in the future.

What can be done to improve management of resources to reduce the impact of the floods, reduce vulnerability and improve conditions for recovery? To mitigate natural calamities caused by the inundation and flooding, it is required to re-establish a figure of historical flooding level in order to find solutions overcoming the consequences of similar flooding in the future. In Vietnam, the establishment of inundation map based on the local topographical map has produced valuable results, but the use of GIS tools to reproduce the historical flooding in 1999 would be the basis to forecast the flooding behaviour corresponding to the different scenarios.

1.2. Framework and context

Some remarkable results have been obtained so far in Vietnam with the use of GIS tools in the flood hazard management. With the technical - financial support by the Dutch government in period 1994-1996, the Center of Sea Hydrometeorology implemented the project of coastal ruin caused by the raise of the sea level. The Remote Sensing Center of the Geology Institute has applied the telephoto and GIS in the mapping of inundation that caused by rains in Hai Duong province during 1996- 1998. The Geography Institute has used GIS method to establish the inundation maps of the plain area of Thua Thien Hue province in period from 1999 to 2000. One of the results of this cooperative program between the Dutch and the Vietnamese Government is the development of the STREAM model.

The RIKZ / Coastal Zone Management Centre of the Dutch Ministry of Water and Transport requested to investigate the hydrology of the Perfume River in Vietnam and the Krishna River in India

with the STREAM water balance model. The results of calibration and validation of the hydrological model that was set up for the wider Perfume River Basin in Thua Thien Hue Province, Vietnam including the rivers Huong, Hue Trach, Ta Trach, Bo and O Lau, have been reported (Aerts and Bouwer 2002). These analyses are the first step of investigating whether the STREAM Perfume water balance model is suitable to reproduce the hydrological behaviour of this catchment area. The Institute of Environmental Studies (IVM) of the Vrije Universiteit in Amsterdam carried out these modelling activities.

Originally the water balance model that is used in STREAM, was developed by Deursen and Kwadijk (1994) for the Rhine basin, called RHINEFLOW. This model primarily assessed the effects of climate change on the hydrological cycle of this river basin. For STREAM the original MS-DOS model was adapted to run under windows environment. Several models have been designed to be added to the original water balance model. For example, the present model available for the Ganges Brahmaputra Meghna basin includes a specific module on salt intrusion to assess the impacts of river basin management on the coastal zone.

Because the STREAM model is a raster-GIS water balance model, the spatial analysis is easier compared with 1D models. The output raster maps shows exactly the area of interest for management proposes. Another advantage of this model is that the script language used is very clear and therefore easy to change by the user to meet special objectives. The script language used is BLAISE.

STREAM (Spatial Tools for River basins and Environment and Analysis of Management options) is an instrument for River Basins studies with emphasis on management aspects. STREAM is built around a spatially distributed water balance model for simulating the hydrological behaviour in larger river basins. The simplified GIS based model allows the analysis of water availability patterns and their changes according to artificial measures (i.e. land uses changes as deforestation and irrigation) and external influences as climate change.

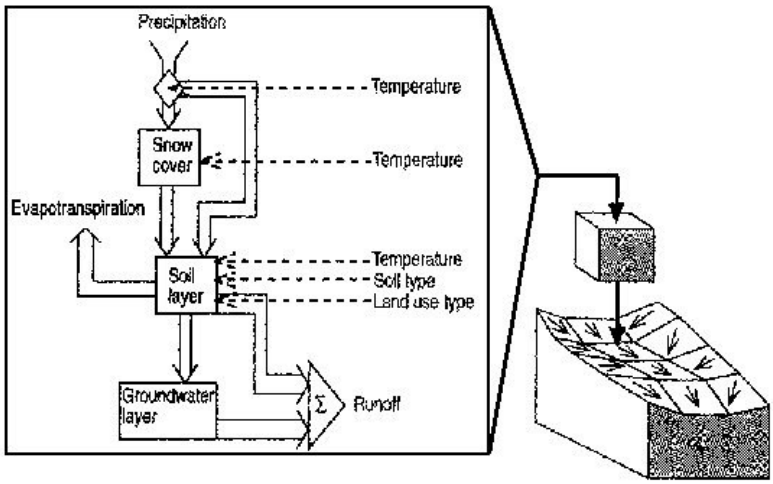

Figure 1. Flow Chart of the Calculations of the STREAM Model

The spatial water balance model is based on a raster GIS calculation for each grid cell of the studied river basin (Figure 1). The direction of the water flow is determined by the digital elevation model (DEM). The first step of the water balance is based in the calculation of the Potential and the Actual Evapotranspiration. The Potential Evapotranspiration (PE) is calculated using the Thornthwaite & Mather empirical equation, which uses Temperature and Day Length estimates as inputs. The PE is calculated using the following expressions:

$$PEi = 16\left(\frac{10Ti}{H}\right)^{A} \quad (1)$$

if $0 \leq T \leq 26.5$ °C or

$$PEi = -415.85 + 32.24Ti - 0.43Ti^{2} \quad (2)$$

if $T \geq 26.5$ °C

where T*i* is the mean surface air temperature in month i (°C) and H is the Heat index. The PE should be corrected for day light duration in the case of daily evapotranspiration and also for the length of the month in days. The next step in the calculations is the balance of the PE with the precipitation (PRE) maps in each pixel and the calculation of the amount of water that could be stored in the soil according to its water holding capabilities. The excess is separated into direct and delayed runoff, and groundwater storage depending of the characteristics of each pixel. The spatial inputs needed to complete the input database and run the water balance model are a Landuse map and a Soil type map. These maps determine the physical characteristics of the soil to retain water or lose it (Aerts, Kriek et al. 1999).

The model originally runs on a monthly basis but the time steps could be changed according to the objectives, the size of the basin, the available data and the configuration of the computer system. In this study the time step was reduced to a daily basis.

STREAM has been proved to be useful to give insight in the long-term impacts of land-use change, climate change, river basin management, population pressure, economic development and on the future water demand and water availability in the Krishna basin. Additionally, STREAM can, contrary to many other hydrological models, give insight in the spatial variation of the changes, and complement research the interaction of rivers with coastal processes. Currently, a team has been set-up by RIKZ / CZMZ and IVM comprising other institutes as well, for a broader application of the STREAM model.

1.3. Purpose of the study

This study focuses on the modeling of the flooding event in November of 1999 with the help of the Stream model and will try to estimate the amount of water coming to the flooded areas in the coastal plain. As a second objective a comparison will be made between the rainfall rates collected in ground station and the Tropical Rainfall Mission (TRMM) information. The best estimator of the total rainfall for the discharge calculation will be selected by comparing with the discharge data collected in the ground. To reach this objective the STREAM model or the Perfume River has to be changed into higher temporal and spatial resolution. A new DEM (with higher resolution than the one used in the model with 1 km of pixel size) and new Landuse and Soil type maps (used to generate the Crop factor and Water holding capacity maps) will be the other input for the model necessary to estimate the discharge rates to the flooded area.

Once the total amount of water coming to the flooded area is calculated, the total area and the height of the water level will be estimated with the help of the DEM assuming a horizontal altitude of the flood. To validate this result and estimate the actual extension of the flooding, three maps were obtained by calculating the flood area from Synthetic Aperture Radar (SAR) Radarsat images obtained just after the flooding peak. This calculated area will be used to estimate the balance between inputs into and outputs from the flooding area using a reservoir model. The goal will be the establishment of a GIS basis for flood management in the TT Hue province in Vietnam by the application of a tool that could be used in probability analysis to model possible flooded areas according to different scenarios of rainfall.

The new DEM, Landuse and soil type maps, as well as the maps based on Radar images, were kindly provided by Research Institutes in Hue, Hanoi and Hai Phong. The gathering of all this information was the main objective of fieldwork in Vietnam during November 2003.

2. Study area

2.1. Location

Vietnam lies in the eastern part of Indochina, bounded by the South China Sea and the Gulf of Tonkin to the east and by the Truong Son mountain range to the west. Extending between latitudes 8-24oN Vietnam is thus effectively entirely within the tropics. Its coastline stretches over 3,260 kilometres.

Vietnam has a tropical monsoon type of climate with frequent tropical cyclones affecting the northern and central regions. They also occur in southern areas but less frequently. The seasonal distribution of rainfall is closely related to the monsoons. Rainfall intensity can be high, producing a rapid rate of runoff and serious flooding. Most of Vietnam experiences an annual rainfall of 1,800-2,500 mm, distributed unevenly through the year. Approximately 70 percent of the rainfall occurs during the main rainy season from May to September/October. The uneven distribution of rainfall is one of the main causes of river flooding.

Because of its low coastal topography, Vietnam is exposed to the high winds and storm surges brought by tropical cyclones. Furthermore, the whole country can be affected by the weather conditions over the ocean to the east. The northwest Pacific Ocean is the principal spawning ground for tropical cyclones which often track through the Philippines and then strike the Indochinese mainland through Vietnam.

Statistics for the 38 years from 1954 to 1991 (Table 1) indicate that the only two months in which no tropical cyclones occurred were January and February. They are relatively infrequent in March, April, May and December. The main cyclone season in Vietnam therefore covers the six months from June to November in which 94 percent occurred in the years under review. Of the total of 225 the highest monthly frequency occurred in September and October, each accounting for 48 of that total. The average annual frequency during the 38 months was 5.9. Regionally, the peak occurrence was in the month of August for the north, October for central and November for the southern region. This shift from north to south is a common feature of the behaviour of Northwest Pacific tropical cyclones with their tendency to track northwards during the early part of the typhoon season and then progressively taking more westerly tracks from their point of generation as the season continues. Obviously there are many exceptions to this tendency. A partial explanation of this fact lies in the sea surface temperatures (SSTs) which decrease later in the season. With a threshold SST of approximately 26oC needed for the generation of a typhoon, by September this is only found in those ocean areas further south where the SST remains around 25-28oC throughout the year. Table 1.1 show the frequency of tropical cyclones in Vietnam during the years 1954-1991 by region.

Table 1 Total numbers of tropical cyclones in Vietnam (1954 – 1991)

Regions	*Jan*	*Feb*	*Mar*	*Apr*	*May*	*Jun*	*Jul*	*Aug*	*Sep*	*Oct*	*Nov*	*Dec*	**Total**
Northern	0	0	0	0	0	15	24	28	22	7	1	0	97
Central	0	0	0	1	2	0	0	14	23	35	6	0	81
Southern	0	0	3	1	1	7	0	0	3	6	20	6	47
TOTAL	0	0	3	2	3	22	24	42	48	48	27	6	225

2.2. Province of Hue

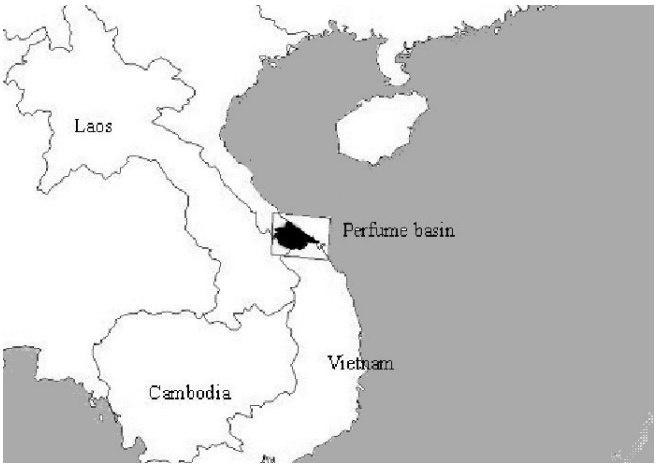

Figure 2. Map of southeast Asia showing Vietnam and the Hue Province

The study area is located in the Center of Vietnam, with its coordinates are from 16°20' to 17°15' of the north latitude and from 107°05' to 108°15' of the east longitude, comprising 2 basins of 4 rivers. For the administrative units, this study area includes 1 city. This is Hue city. The Huong river (Perfume River) is the greatest river of the Thua Thien Hue province and located from 16°00' to 16°45' of the north latitude and from 107°00' to 108°15' of the east longitude, its west is the Truong Son mountains, its north is Bach Ma mountains, its south is contiguous to the Da Nang city and its east is Dong sea

The most general topographic form of the study area is the mountains in the west and the sea in the east. A narrow delta is located immediately the east side of the Truong Son mountain range and cut into many small plains. The central coastal plains were formed by the combination impact of the rivers and the sea. In regard to their origin, they involve closely the adjacent mountainous area in the west. The east edge of these plains is the seaside. These plains are a stretch land whose soil is mixed by alluvium from the mountains and sea sand. These plains are allocated as a chain along to the east side of the Truong Son mountain range.

The Huong river has a basin area of 2,830 km2 that representing 56% of total area of Thua Thien Hue province and playing an important role on water resource as well as the inundation status of the province. Over than 80% of this basin area is hills and mountains with their heights from 200 to 1,708 m (the Mang peak of the Bach Ma range), and tens peaks with their height are more than 1,000 m which scattered in the area. A 5% of the basin area is the coastal dunes with altitude from 4- 5m to 20-30m, the remainder area is 3,700ha which can be cultivatable. In general, the area topography is gradually lowered from the north west to south east. The Huong river basin is developed strongly in its left bank: the left bank area is more twofold than the right bank area. The small river and streams in the left bank, the main river upstream and the Huu Trach river are quite slope.

2.2.1. System of rivers and streams

The Huong river basin (Perfume River) covers the majority area of the Thua Thien Hue province that located in the east of Truong Son mountainous range and in the north of the Bach Ma range. Its main flow originates from a high mountain area of the Bach Ma range where is from 900 to 1,200m of altitude. From its origin to the Tuan cross-river, the main flow is called as the Ta Trach and from the Tuan cross-river, it is called as the Huong river (or Perfume river), the river that expresses many bold romantic feature on life, culture and natural landscape of the Hue ancient capital.

The main flow of the Huong river has a length of 104km. The river stream system, if counting for the different subflows longer than 10km, has 5 subflows in class I, 12 subflows in class II, 1 subflow in class III and 1 greatest subflow which called as the Dai Giang river has a length of 27km. Three greatest subflows counting from their origins are as follow : the Ca Rum Ba Ram river lies in the right of the main river with a length of 29km, a catchment area of 219.3 km2, and its confluence is 77km from the estuary of the main river. Two subflows lying in the left of the main river are: the Huu Trach river with a length of 50km, a catchment area of 729 km2, and its confluence is in the Tuan cross-river with a distance of 34km from the estuary of the main river; the Bo river with a length of 94km, a catchment area of 938km2, and its confluence is in the Sinh cross-river with a distance of 9km from the estuary of the main river.

The Huong river water converges in the Tam Giang- Cau Hai lagoon that is of 67 km long, average width is of 2.2km and its depth changes from 1- 5m, and then goes to the sea through mainly the Thuan An estuary (before the flood in October 1999; plus the Hoa Duan and Tu Hien estuaries (after the flood in November 1999).

2.2.2. Temperature and humidity

The Huong basin has a quite high temperature extent with annual average temperature changes from 21 to 26^{o}C. The maximum temperature occurs normally in June, July and August, while the min. temperature occurs in November, December and January. The highest temperature in the Hue city is 41,3^{o}C and in Nam Dong is 39,7^{o}C.

The relative humidity in the Huong basin is rather high; the average humidity in many years attains 84- 85%. In July, the humidity is lowest (only 50- 60%), while in November and December is high (higher than 90%), with drizzle during many days.

2.2.3. Wind, storm

In the Huong basin, every year has two main wind seasons: southwest wind and north east wind. Southwest wind begins from March and is current from May to July. Southwest wind blows through the Truong Son mountain range and has a “” effect that makes dry hot and causes frequently drought in dry season. Northeast wind begins from September, prolongs to March, April in next year. Due to influence of the Truong Son and Bach Ma mountains, northeast wind causes normally rains and dry cold weather.

The Huong basin situates in a zone that suffers largest influence of storms. According to the statistic data in more 30 last years, the number of storms landed on Quang Binh- Thua Thien Hue region representing about 27% of total number of storms that affected on our country. The highest wind speed attained teens m/s (In Hue : 28 m/s, in A Luoi : 40 m/s and in Nam Dong : 25 m/s).

2.2.4. Rainfall, evaporation

The Huong basin rainfall is ranked in one of the high levels in the country. The annual average rainfall of the total basin is 3,200 mm, occurring the highest rainfall in October, while lowest rainfall is in February.

2.2.5. Hydrologic characteristic

The river flow distribution is irregular in accordance with the rainfall distribution. The flood season prolongs from October to December and its water quantity represents from 50 to 80 per cent of total annual water quantity, and changes strongly year by year. The water quantity of flood season in a year having many floods may be threefold the water quantity in another year having fewer floods. Its flow module varies largely in flood season and dry season. In Thuong Nhat hydrologic station, the flow module changes averagely from 18.5 l/skm^2 (in dry season) to 228 l/skm^2 (in flood season).

2.3. Flood plain

The coastal area of the Hue province is dominated by a system of lagoons. The principal lagoon is the Tam Giang. The Tam Giang Lagoon (see), which runs along the coast of Thua Thien Hue Province, Vietnam, has an area of 22,000 ha. On its eastern side, the lagoon is separated from the sea by sandy dunes with two openings, Thuan An and Tu Hien. On the western side of the lagoon are rice fields and river estuaries. The area is unique in terms of landscape and biological resources. Communities settled there to exploit the lagoon's biological resources and farm on the sandy land at its edge ((Phap and Thuan 2002)

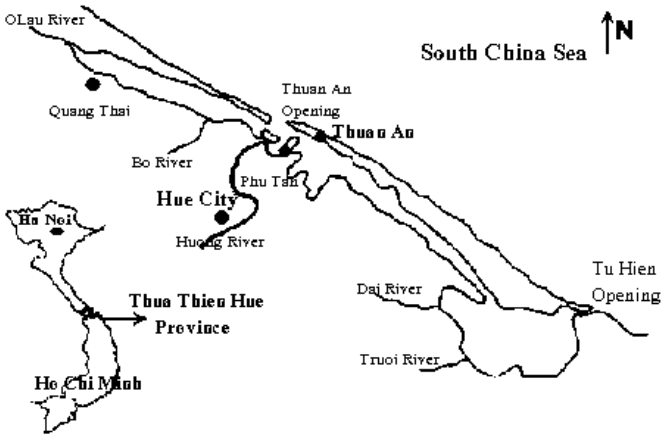

Figure 3. Tam Giang lagoon and the affluent rivers

Because of its minimum slope and high amount of water coming from rivers and from direct rain, this area has a high probability of floodings. This is even enhanced because the sandy reefs, located in the border with the sea, have heights up to 20 m. This causes a difficulty to the water to flow freely in the case of severe flooding making this area behave like a reservoir.

2.4. The Flooding Event of November 1999

During the first two weeks of November 1999, six provinces in central Vietnam experienced the heaviest rainfall and flooding to hit the region in 40 years. The provinces of Quang Binh, Quang Tri, Thua Thien-Hue, Quang Nam, Quang Ngai, and Sing Dinh, as well as the city of Da Nang, were most severely affected by the Tropical Storm (TS) Eve (Joint Typhoon Warning Center - JTWC).

(a) **(b)**

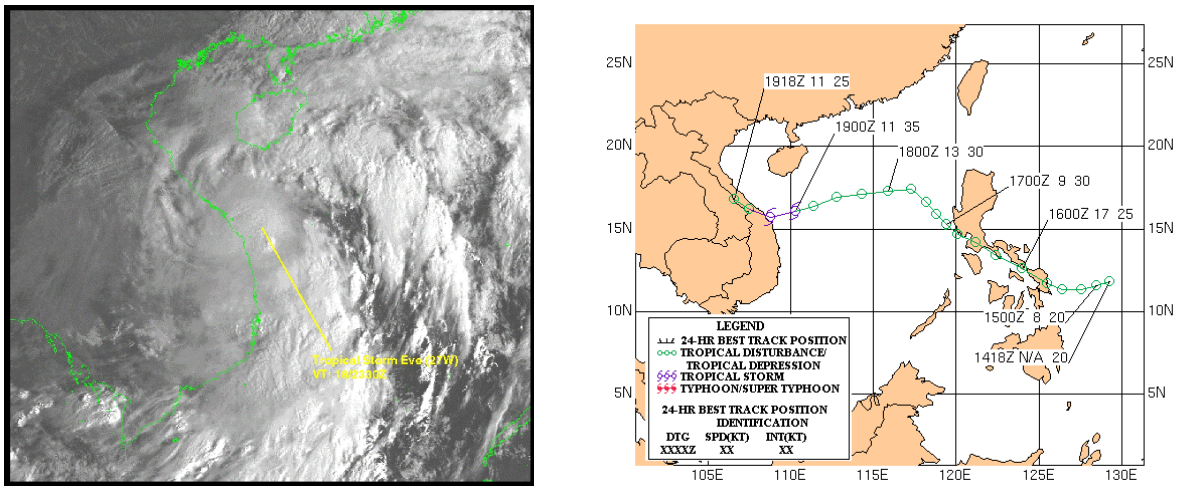

Figure 4. (a) GOES satellite image of the Tropical Storm "Eve" and the Southeast coast line of Asia (in green), (b) Track of the storm obtained from the Naval Pacific Meteorology and Oceanography Center (NPMOC) and Joint Typhoon Warning Center (JTWC) Support Web.

The TS Eve (Figure 4a) was initially detected northeast of Mindanao as a poorly defined low level circulation center with disorganized convection. As organization increased, a TCFA was issued at 150230Z October followed by the first warning at 150900Z October with a 25 kt intensity. Afterward the TS Eve tracked northwestward across the Philippine Islands as a tropical depression. After the cyclone moved over the South China Sea, it turned toward the west, and then west-southwest as low to mid-level ridging built north of the system from southeastern China. During this period, the cyclone also intensified into a minimal tropical storm reaching a maximum intensity of 35 kt at 190000Z October (Figure 4b).

The TS Eve (27W) made landfall at 190600Z October, 60 nm southeast of Da Nang, Vietnam, as a minimal tropical storm (35 kt) and the cyclone quickly dissipated over land. JTWC issued the 18th and final warning at 191500Z October as it moved inland and dissipated.

Vietnam experienced the worst effects during this landfall. First perceived in the downpour from 18 to 20 October 1999, “Eve”, lashed Vietnam's central provinces. The effects of Eve's torrential rainstorms far exceeded the expected norms of seasonal flooding; dangerous (level II) and very dangerous (level III) flood conditions prevailed in the valleys of several major rivers in the central provinces.

By 1st November rivers in the provinces stretching from Nghe An to Binh Dinh exceeded alarm level III. Uncontrollable flooding combined with landslides inflicted severe damage on roads, dykes and infrastructure. The level of the Huong River (Perfume) in Hue reached approximately 5.6 m, thus overreaching its historic 1983 flood level by 8 m. The streets of Hue ran with water up to 3 metres high. Equally, the Vu Gia River in Quang Nam, and major rivers in Quang Tri, Quang Binh and Binh Dinh outstepped manageable limits.

The harsh weather conditions began to show some signs of abating on 4th November, though upstream rains continue. River levels have descended, but still fluctuate. At 1.00 p.m. on 4 November, the Huong River at Hue Guaging station measured 3.81 metres; that evening, waters rose to 4.14 m at the same point, and today's measures indicate a height of 4.36 m above the norm.

On 5th November the Central Committee for Flood and Storm Control (CCFSC) reported at least 233 deaths resulting from more than a fortnight of flooding in central Vietnam. It is known that approximately 255,299 houses collapsed and 15,000 households were evacuated. At least 6,477 ha of paddy fields were damaged by the deluge.

The international help consisted of tons of food for the more of 300,000 evacuated persons from the central provinces.

3. Methodology and data

This chapter provides a description of the methodology that will be followed to obtain and process each input data to make it appropriate for the STREAM model to run and estimate runoff amounts. A description and a preliminary analysis of selected meteorological and hydrological datasets for the River Basin in Thua Thien Hue Province will be also made.

3.1. Model configuration

Stream is GIS based model, so that means that all the input data should be raster maps, in the same format and having the same georeference and spatial resolution.

3.1.1. Format

The raster images were all calculated, imported and georeferenced in ILWIS 3.2 because of its friendly interface but the STREAM model can read only raster images in IDRISI 32 format. For that reason all the images had to be transformed into this format. IDRISI is a geographical analysis and image processing software developed by Clark Labs.

The files of the IDRISI 32 format (32 bits) have the extension "*.rst" and the accompanied metadata file "*.rdc". To transform the files from ILWIS format the export command was used and the IDRISI.IMG format selected. These files have the old 16 bits format, so, they had to be transformed in IDRISI into 32 bits format using the Idrisi file conversion (16/32) command.

3.1.2. Georeference and Spatial resolution

Most available source data in Vietnam is in Universal Transverse Mercator (UTM) 48N projection, WGS84 Ellipsoid and WGS 1984 Datum. Therefore, for practical reasons, it was decided to make this the standard projection. The following are the parameters of this chosen projection

Projection used	=	UTM 48N
Units	=	meters
Pixel Size	=	300 meters
Radius of Sphere	=	6,371,007 meters
Min X	=	713330.8
Min Y	=	1766093.1
Max X	=	848491.1
Max Y	=	1856660.4

The spatial resolution was established in 300 m because of the model performance. The model needs virtual memory to store temporally the calculations and with the higher the resolution of the database the more need of memory is. The other factor that was considered was the time consuming. With

database of 300 m, the model takes 8 minutes approximately to run in a Pentium 4 computer with 512 Mb of RAM memory and 1,8 GHz of processor speed. In the case of a database with 30 m. of spatial resolution it will take 10 x 10 = 100 times more (800 minutes) to make the same calculation for the same area.

3.1.3. Creating the input maps

The model needs the following initial input (in italic the source of the data):

MASK: the whole basin. *Based in Hue province boundary*
Covermap map used to mask the basin area. *From MASK*
BPGLDD: discharge direction of cell. *From DEM*
C: a calibration parameter. *Initial value = 3*
APWL: the accumulated potential water loss (mm water). *Iterative*
GW: the groundwater capacity. *Iterative*
SNOW: the initial thickness (mm water) of the snow cover. *Not considered*
SOILSTOR: the soil storage of water. *Iterative*

The following daily climate data input (in italic the source of the data):

TMP: the temperature (average temperature in the month in °C). *From meteorological data*
PRE: the total precipitation in the month (mm)). *From meteorological data*
HEAT: parameter (constant) used to calculate PE. *From TMP (Temperature)*
A: parameter (constant) used to calculate PE. *From TMP (Temperature)*
DAY: the length of a day (hours of sunshine). *From Old data*

Thie following mas are used to complement the water balance model

CROPF: crop parameter, which reflects the effect of crop on the PE. *From Landuse (see Landuse section 3.3.*
WHOLDN: the water holding capacity of the soil. *From Soiltype (see Landuse section 3.3.*

Internally the following variables are used:

SNOW1: the amount of snow fallen (mm water) Not calculated
SMELT: the amount of snowmelt (mm water) Not calculated
EVEN: temporary variable
PE: the potential evapotranspiration (mm water)
PEFF: the effective potential evapotranspiration (mm water), PRE - PE
AE: the actual evapotranspiration
TOGW: the flow to the groundwater
SSTOR: the soil storage of water (available for evapotranspiration) (mm)
RUNOFF: the quick flow; fast runoff (mm)
SLOFLO: the slow flow; from the groundwater (mm)
DSCHRG: the discharge for the cell (mm)
DISMM: total discharge in the cell with discharge from all contributing cells (mm)
DISQSEC: discharge in m3 per second
DISTEMP: variable used to stretch DIS maps (if < 40 then 0)
DISTEMP2: variable used to stretch DIS maps (if > 5000 then 5000)

The following maps are exported for each month:

ARID:	aridity index (actual evapotranspiration / potential evapotranspiration) (-)
SNOW:	the amount of snow (mm water) not calculated
DISCHRG:	the discharge for the cell (mm/month)
DISQSEC:	discharge map (m3/sec)
TMP:	Temperature map
PRE:	Precipitation map

All the parameters are exported for each month in graph form

3.1.4. Mask and COVER map

The mask itself is derived from the province boundary (Figure 5), that was provided by the Viet Nam Netherlands Integrated Coastal Zone Management (VN–ICZM). The basin (mask) has the following characteristics:

Cellsize:	300 m
Rows:	303
Cols:	452
Min X	713330.8
Min Y	1766093.1
Max X	848491.1
Max Y	1856660.4

This corresponds to 136956 cells of 300 x 300 m (which is 12326 km^2).

Figure 5. Hue Province Boundary used to make the Mask and Cover maps.

With the aid of ILWIS, the appropriate basin has been cut out. The following procedure is used: The shapefile is rasterized with the same cell size and characteristics previously specified. In this way two images are calculated: the MASK and the COVERmap. After some reclassification the basin mask has a value of 0 (basin) and -9999 (outside basin). The COVERmap has a value of 1 (basin) and 0 (outside basin).

3.1.5. Elevation map, DEM derivation and Flow direction BPGLDD

The Elevation map with contour lines, digitized from Topographic maps, was obtained from the CCP project and the Institute of Geography in Hanoi. The topographic maps had a 1: 50,000 scale and were originally published by the Land Register Service of Vietnam from 1993 to 2000 and lying in the HANOI-72 reference system and the GAUSS grid. The vertical resolution of the Elevation map is of

2.5 m. in the range of 0 and 10 m, 10 m up to 40 m and 20 m up to 1780 m that is the highest contour line of the topographic map.

The Digital Elevation Model (DEM) was generated from contour interpolation, from the digitised contour lines on the topographic map, by ILWIS software with a pixel resolution of 30 x 30 m. This DEM was used in the flooded area estimation once the discharge data from STREAM was obtained.

(a) **(b)**

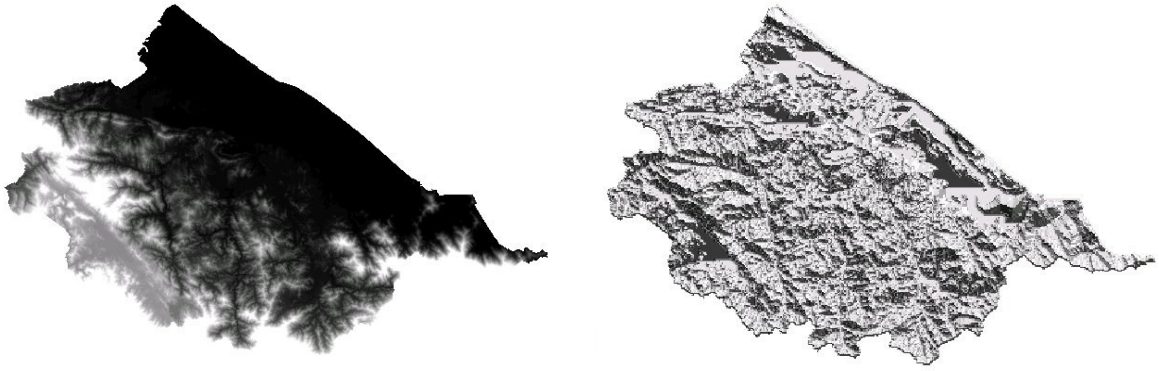

Figure 6. Images derived from elevation map: (a) DEM with 30 m resolution and (b) flow direction map with values between 1 and 9.

This DEM once derived (Figure 6a) was resampled to a lower resolution map at a pixel resolution of 300 x 300 m like the rest of the STREAM inputs. The STREAM does not use the DEM image as it, but a flow direction map. With the lower resolution DEM, the flow direction map was calculated in IDRISI with the FLOW command in the GIS analysis – Surface analysis menu. This image has the flow direction values by pixel in degrees (between 0° and 360°) but the model uses only values between 1 and 9. The values were reclassified using the classes shown in the Table 2 with the RECLASS command in IDRISI.

Table 2. Reclassification of the flow direction map in IDRISI 32

Class	To values from	To
8	337.5	361
8	3	22.5
9	22.5	67.5
6	67.5	112.5
3	112.5	157.5
2	157.5	202.5
1	202.5	247.5
4	247.5	292.5
7	292.5	337.5

After the classification the pixel values had the following configuration according to the direction of the flow. The value 5 means no direction of the flow.

7	8	9
4	5	6
1	2	3

The flow direction map (BPGLDD) is shown in the Figure 6b as it will be used in STREAM.

3.1.6. C Parameter

C is a calibration parameter, so the C map is created in the calibrating procedure of STREAM. For the Perfume basin a value of 3 for the whole basin has been chosen as initial value. Generally this is a good estimate to begin with. When the C parameter is increased, the peak of the discharges in the hydrograph is reduced and more water is added to the tail raising it. The contrary is observed in the case of low C. Once the results from the first run of the model are obtained, the C parameter should be changed until the best estimate fits the calibration.

3.1.7. Iterative maps

The Init maps (APWL, GW, SNOW and SOILSTOR are all calculated iteratively with the exception of the SNOW map that is calculated in the original model but for this model was not considered because the area belongs to a tropical country with no occurrence of snow precipitation and melting process.

At the beginning of the run (day 1: 15th October) the images have values of 10 but they are changed daily according to the internal calculations. Another approach is to run the model for the period of modeling (32 days) and copy the final values (day 32: 15th November) to the initial input (day 1). We can see the results that by observing the TSummary of either GW or soil storage maps.

3.2. Meteorological Data

The meteorological dataset consisted of hourly rainfall, temperature and river water level in stations of the catchment area of the Perfume River for the period 15 October to 15 November 1999 (see) were provided by the Hydrometeorological Service of Vietnam (HMS) and Mr. Lie (University of Hue). These data were delivered through the Viet Nam Netherlands Integrated Coastal Zone Management (VN–ICZM) project office in Hanoi. An analysis was preliminary carried out before the calibration of the STREAM water balance model. The complete tabular meteorological database is shown in the Appendix 2. With the rainfall and temperature data the maps PRE and TMP respectively were calculated. With the TRMM data another set of precipitation maps were estimated and used separately in another STREAM run. The objective of this was to compare the results of the ground collected and the satellite based rainfall data as it was established in the introductory chapter.

3.2.1. Station locations

The hourly data of precipitation and temperature, for Nam Dong, A Luoi and Hue meteorological stations, and water levels and discharges for the Phu Oc, Kim Long and Thuong Nhat hydrological stations, were obtained. The locations of the meteorological and hydrological stations within the basin are shown in the Figure 7

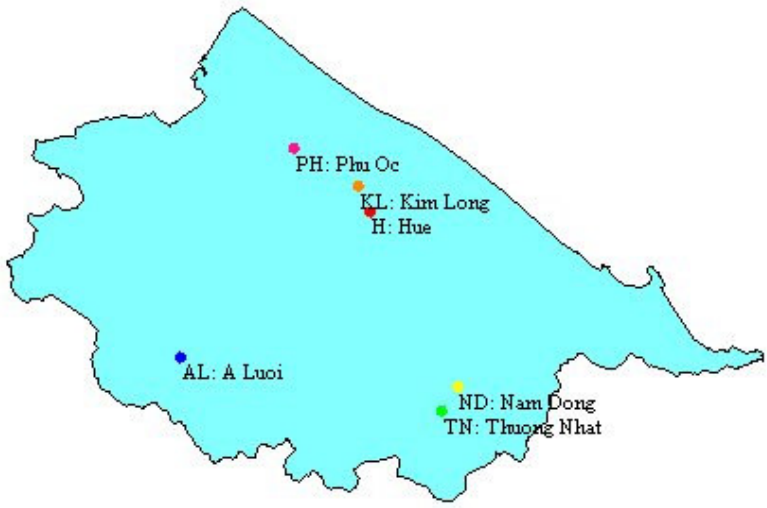

Figure 7. Geographical location of the Meteorological Stations in the Catchment area

The geographical coordinates of the stations are showed in the Table 3 and Table 4. The original Lat-Long geographical coordinates were changed to the projection UTM 48 N to make them compatible with the rest of the raster maps. The meteorological stations table was the base to build point maps for the ground collected precipitation and temperature input of the model in.

Table 3. Location of the Meteorological Stations

Station	***Altitude (m)***	***Lat-Long Coordinates***		***UTM coordinates***	
		Latitude	*Longitude*	*Easting*	*Northing*
Hue	18	16°.26'	107°.35'	775870	1818629
Nan Dong	52	16°.10'	107°.43'	790510	1818629
A. Luoi	580	16°.13'	107°.17'	744087	1794260

Table 4. Location of the Hydrological Stations

Station	***Altitude (m)***	***Lat-Long Coordinates***		***UTM coordinates***	
		Latitude	*Longitude*	*Easting*	*Northing*
Phu Oc	5	16°.32'	107°.28'	763269	1829544
Kim Long	10	16°.27'	107°.33'	772285	1820429
Thuong Naht	81	16°.07'	107°.41'	787422	1784481

3.2.2. Precipitation

The Figure 8 describes a 30-days record of daily rainfall at the three meteorological stations. A peak during the period between 1 and 6 November is observed that corresponds to the time when the typhoon passed by the study area.

The maximum was recorded in the Hue station (in the city) on November the 2nd when 1048 mm of rainfall was registered. Previously, during the period between 18 and 25 of October, heavy rains were recorded in the catchment area.

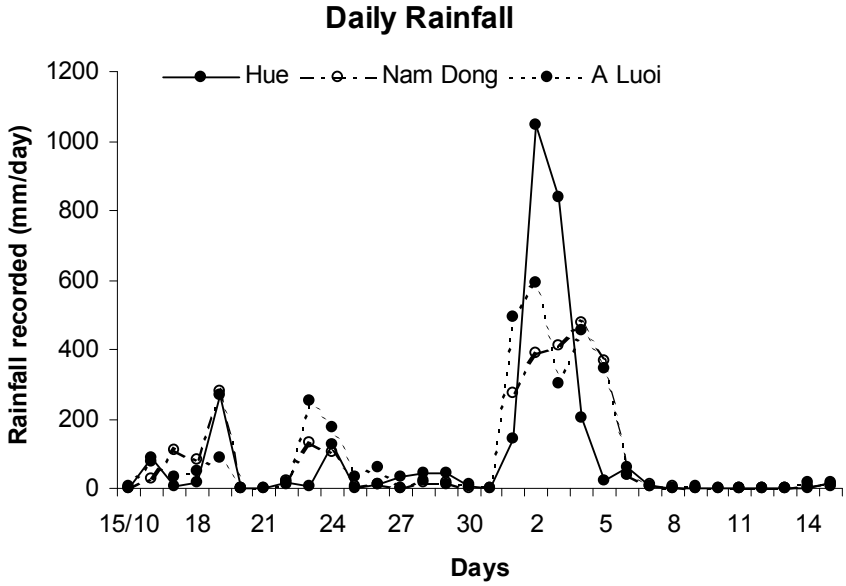

Figure 8. Daily Precipitation recorded at the Meteorological Stations in Hue

3.2.3. TRMM Data

The Tropical Rainfall Measuring Mission (TRMM) is a joint mission between the National Aeronautics and Space Administration (NASA) of the United States and the National Space Development Agency (NASDA) of Japan. The TRMM sensor has been acquiring data from shortly after its launch on November 28th 1997 to the present (Rui, Teng et al. 2002). The objectives of TRMM are to measure rainfall and energy (i.e. latent heat of condensation) exchange of tropical and subtropical regions of the world (between 40°N and 40°S). The primary rainfall instruments on TRMM are the TRMM Microwave Imager (TMI), the precipitation radar (PR) and the Visible and Infrared Radiometer System (VIRS). The space segment of TRMM is a satellite in a 350-km circular orbit with a 35° inclination angle.

The combination of satellite-borne passive and active sensors in the TRMM provides critical information regarding the three-dimensional distributions of precipitation and heating in the Tropics (Simpson, Kummerow et al. 1996). Coincident measurements TMI and PR are complementary: passive microwave radiometers measure radiances that are the end product of the integrated effects of

electromagnetic absorption-emission and scattering through the precipitating cloud along the sensor viewpath.

The TRMM is based in the fact that clouds are opaque in the VIS and IR spectral range and precipitation is inferred from cloud top structure. At passive MW frequencies precipitation particles are the main source of attenuation of the upwelling radiation. MW techniques are thus physically more direct than those based on VIS/IR radiation. The emission of radiation from atmospheric particles results in an increase of the signal received by the satellite sensor while at the same time the scattering due to hydrometeors reduces the radiation stream. Type and size of the detected hydrometeors depend upon the frequency of the upwelling radiation. Above 60 GHz ice scattering dominates and the radiometers can only sense ice while rain is not detected. Below about 22 GHz absorption is the primary mechanism affecting the transfer of MW radiation and ice above the rain layer is virtually transparent. Between 19.3 and 85.5 GHz, the common passive MW imagers' frequency range, radiation interacts with the main types of hydrometeors, water particles or droplets (liquid or frozen). Scattering and emission happen at the same time with radiation undergoing multiple transformations within the cloud column in the sensor's field of view (FOV). At different frequencies the radiometers observe different parts of the rain column.

The TRMM database is freely downloadable from the Internet at the website http://daac.gsfc.nasa.gov of the Distributed Active Archive Center (DAAC) of the Goddard Earth Sciences (DISC) as part of the NASA's Earth Science Enterprise (ESE). There are several types of products available depending of the level of the processing with algorithms to extract rainfall parameters. The level 1 product group are crude calibrated data of radiances of the visible sensors, microwave derived brightness temperature, 3-D distribution of rainfall derived from scanner radar and converted reflectivity factors. The resolution of the pixels ranges between 2.2 and 5 km. The level 2 generates vertical profiles of hydrometeors from brightness temperatures records and the radiometric data with dynamic cloud models. In the 2A12 product, for each pixel the algorithm assigns a surface type (land/ocean/coast) and a freezing height; and computes surface rain, convective surface rain, and profiles of hydrometeors (cloud liquid, cloud ice, water vapor, etc.) at 14 vertical levels. The products of the level 3 consist of final products of global daily and monthly precipitation with lower resolution (from 1° x 1° to 5° x 5° degrees). For this study level 2A12 products were used. Each file contains data corresponding to one complete orbit in HDF format.

TRMM 2A12 algorithm explores the application of profiling techniques ((Kummerow, Hong et al. 2001)) to TRMM microwave imager (TMI) data. Each data granule consists of two parts: metadata and swath data that permits to geolocate each data point. The profiling techniques use the Goddard Cumulus Ensemble Model, and generate vertical hydrometeor profiles on a pixel-by-pixel basis. The top of each layer is given at 0.5, 1.0, 1.5, 2.0, 2.5, 3.0, 3.5, 4.0, 5.0, 6.0, 8.0, 10.0, 14.0, and 18.0 km above the surface. The surface rainfall (in mm/hour) and the associated confidence indicator are also calculated..

Both version 4 and version 5 of TRMM 2A-12 data are available at DAAC. Unfortunately there are two known deficiencies in the version 4 TRMM 2A-12 data. The rainfall rates were affected by the calibration problems in TMI level 1B data, and the latent heat parameter of the algorithm was not reliable. The version 5 of TRMM 2A-12 algorithm has fixed this calibration problem. TRMM scientists are also working on the discrepancy in the rainfall climatology between TMI 2A12 and

TRMM Precipitation Radar data. 2A12 data produces rainfall climatology about 20% higher than PR. The coming version 6 is expected to improve this.(Kummerow, Simpsom et al. 2000). Despite of this disadvantage the surface rainfall records were used as rain rates for this study.

The data collected from DAAC used in this study corresponds to all the available 2A12 orbit files that passed over the study area during the period between 15th October and 15th November. The complete list of files used is detailed in the Appendix 7.2.3. As it is observed there were dates when 2 orbits passed over Hue in only one day and dates when there were not passes at all.

The files were visualized with the Orbit Viewer software (Figure 9) that is freely downloadable from the DAAC webpage and exported to ASCII format as tables. The complete procedure to process the downloaded files is detailed in the Each table had the rain rate data and the respective Lat-Long position. These coordinates were then transformed to the UTM projection.

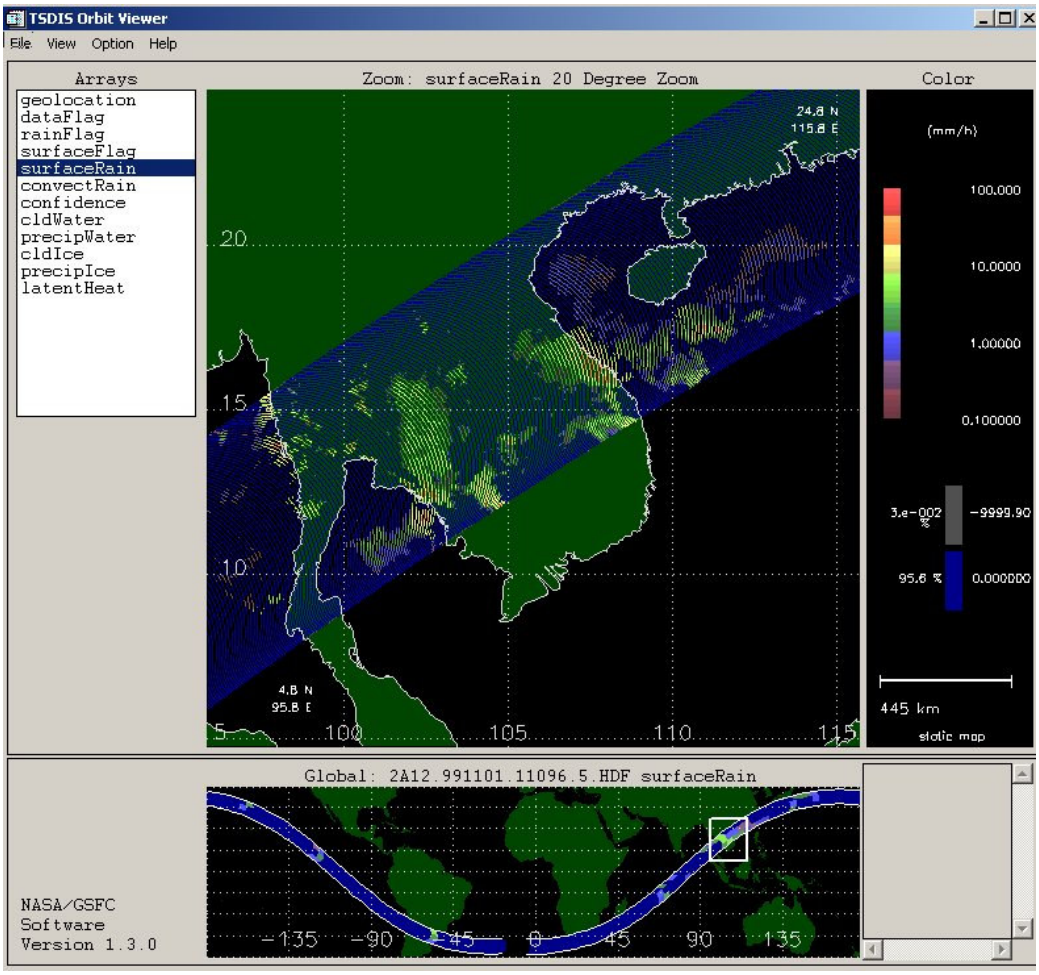

Figure 9. Orbit Viewer window showing an orbit passing by the Study area the 1st November 1999.

This data was then imported as tables in ILWIS to make point maps as it is shown in the Figure 10a. with a map made from data collected the 1st November during the onset of the typhoon. After that, a simple interpolation (Moving Average) of these points was performed and raster images with rain rates were obtained (Figure 10b). Due to the fact that the rainfall rates of TRMM are measured in

mm/hour an adjustment was performed with the ground collected data to obtain daily rates. The daily ground stations records were plotted vs. the TRMM hourly data multiplied by 24 at exactly those points and a linear regression was obtained. The graphs with the plots are shown in Figure 11 and the regression equations are shown in the
Table 5. Then the TRMM hourly grids were adjusted following the linear regression formula and daily rainfall maps were obtained. For the days that no TRMM data was available the rain gauge interpolation maps were used.

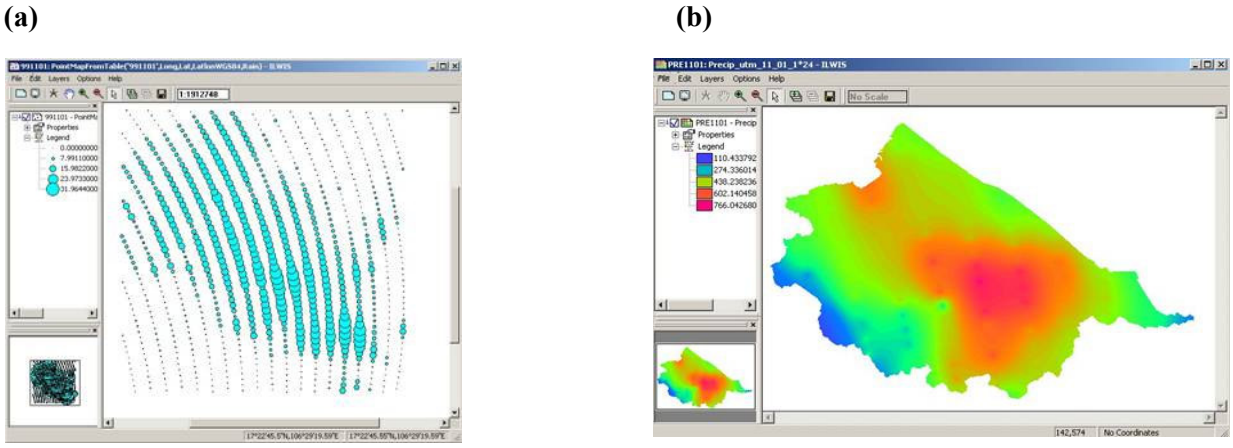

Figure 10: (a) Point Map made in ILWIS with the data extracted from TRMM files and (b) Moving Average Interpolation made from the points. Data corresponding to 1st November.

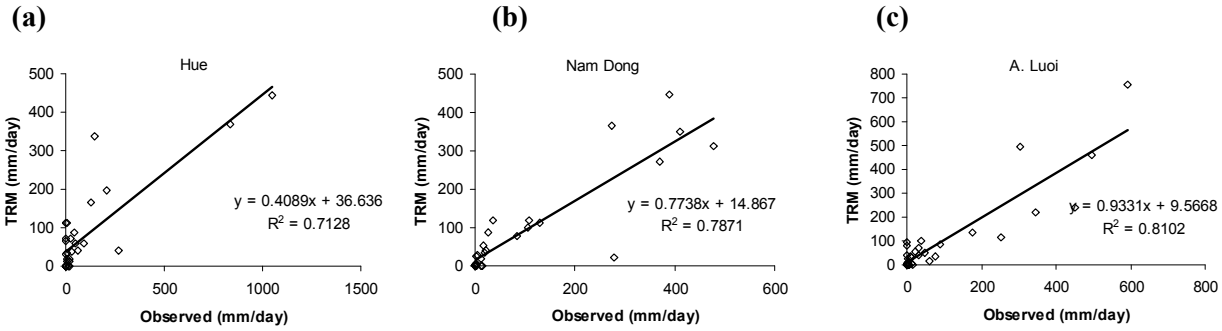

Figure 11. Daily ground stations rainfall records vs. TRMM data at (a) Hue, (b) Nam Dong and (c) A. luoi stations. The daily TRMM data estimations are the hourly values multipied by 24.

Table 5. Results of the regression of the daily ground rainfall and hourly TRMM data

Station	UTM Coordinates (m)		Regression formula	Regression Coefficient (R^2)
	Northing	Easting		
Hue	1818629	775870	Estimated = 0.409*Observed + 36.64	0.71
Nam Dong	1789289	790510	Estimated = 0.774*Observed + 14.87	0.78
A. Luoi	1794260	744087	Estimated = 0.933*Observed + 9.57	0.91

3.2.4. Temperature

The temperature measurements with 0.1 of precision for the three meteorological stations are shown in the figure D. The trend shows a sudden decrease of the temperature during the storming conditions, during the period between 1 and 6 November when the typhoon reached the coasts of Vietnam.

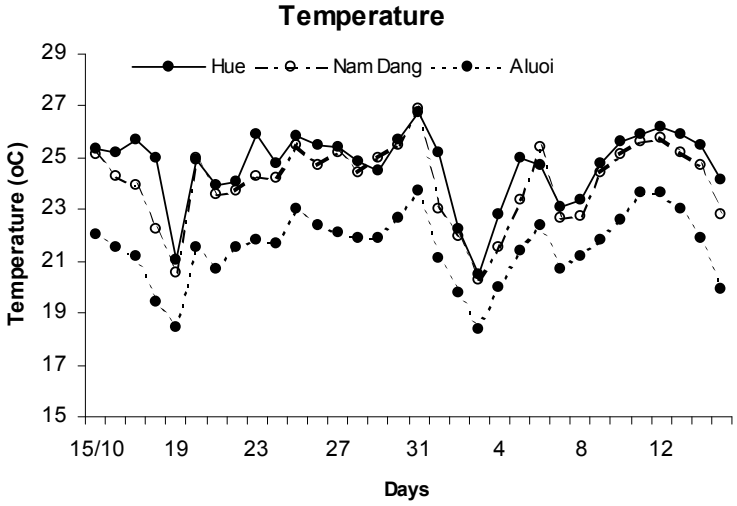

Figure 12. Daily Temperature records at the three meteorological stations in Hue

3.2.5. Discharges

This data was not used directly in the model as input data. Instead, they were used in the calibration of the results from the model. The discharges data was collected from three hydrological stations. The data was recorded as water level in the stations at Phu Oc and Kim Long and as $m^3 s^{-1}$ at Thuong Nhat. The water level is considered as the level above the national datum, ND.

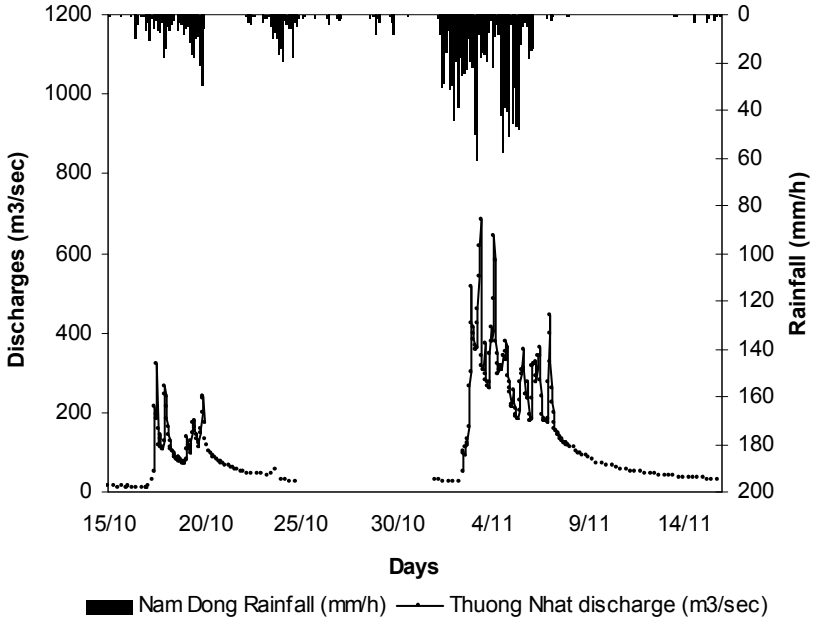

Figure 13. Rainfall records in Nam Dong and discharges at Thuong Nhat station.

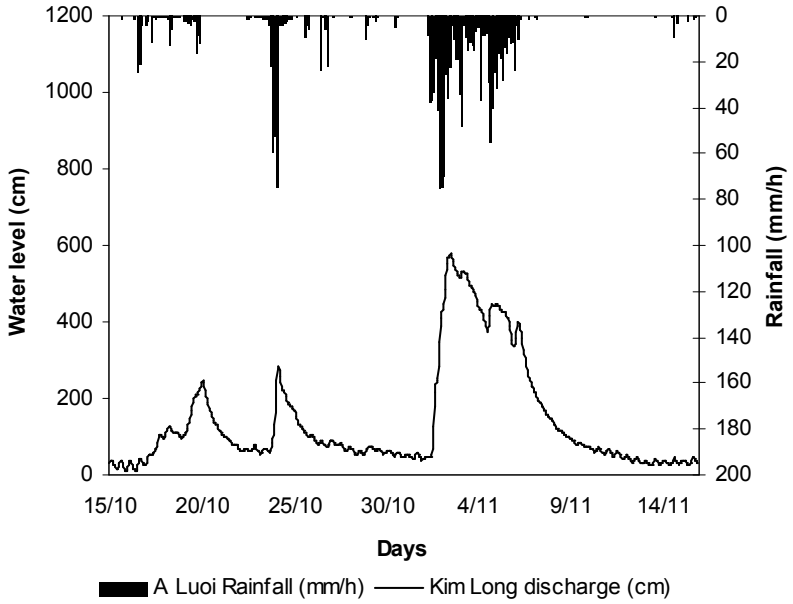

Figure 14. Rainfall records at the A Luoi and the discharge at Kim Long stations.

The Figure 13 shows the hourly precipitation and response in discharge of the Ta Trach River at the station of Thuong Nhat between October 15th and November 15th compared with the rainfall records at the Nam Dong station. The figure also shows the rainfall records at the A Luoi station and the discharge response at Kim Long station. The discharge in this station was registered as height of the river level. The discharge curve shows a very fast response of the Perfume River at the station of Kim Long. The three peaks in the water level curve in Hue follows the main precipitation pattern in A. Luoi. However, the exceptional heavy rainfall in Hue city largely contributed to the enormous increase of water level in the Perfume River of 5.5 m in a few hours time.

It can be seen in Figure 13 that the onset of the increase of the water levels in Hue has a lag of approximately 9 hours with respect to the onset of the precipitation in the mountains at A Luoi station. This leads to the conclusion that the water that falls in the mountains reaches within ~9 hours the city of Hue. The contribution of rainfall in Hue city and in the coastal areas, however, must not be disregarded.

3.2.6. Heat and A

The **HEAT** index and the **A** exponent maps are derived from the processed TMP maps. HEAT and A is calculated using the equations:

$$H = HEAT = \sum_{Jan}^{dec} \left(\frac{T_m}{5} \right)^{1.514} \tag{3}$$

$$A = 0.49239 + 0.01792 \cdot H - 0.0000771771 \cdot H^2 + 0.000000675 \cdot H^3 \tag{4}$$

where:

Tm: Is the mean monthly temperature of the air (°C)

The formulas 3 and 4 are used in the Thornthwaite equation (Equations 1 and 2 in the Introduction Chapter) for the calculation of the evapotranspiration. The calculations were made in ILWIS from the Temperature maps, so they have the same characteristics as the TMP maps and thus automatically the right projection, coordinates and resolution.

3.2.7. Day Length

The length of sunshine hours was obtained from the values of the database used in the original Perfume model. These are 12 values corresponding to hours of sunshine during one day for each month. For the present model the values of October and November (11.64 and 10.92 respectively) were considered in the model. In this way 32 maps with these values for the entire catchment area (17 of October and 15 of November) were calculated.

3.3. Landuse and Soil type maps

The landuse and soil type digital maps were provided by the Institute of Geography of Vietnam in Hanoi. These maps are all in the same projection of the Elevation maps. The Landuse and soil type maps were used for the calculation of the Crop Factor and the Water Holding Capacity maps respectively by applying to each class its respective index. The Landuse - Crop Factor maps, and the Soil Type - Water Holding Capacity maps are shown in Figure 15 and Figure 16, respectively, with their tables of conversions. The tables with the indexes used were provided in the STREAM model manual according to (Deursen and van Kwadijk 1994). Regarding to the Water Holding Capacity, these values should be considered as maximum values. These numbers were estimated, no acurate data was available to link soil type to the maximum water holding capacity

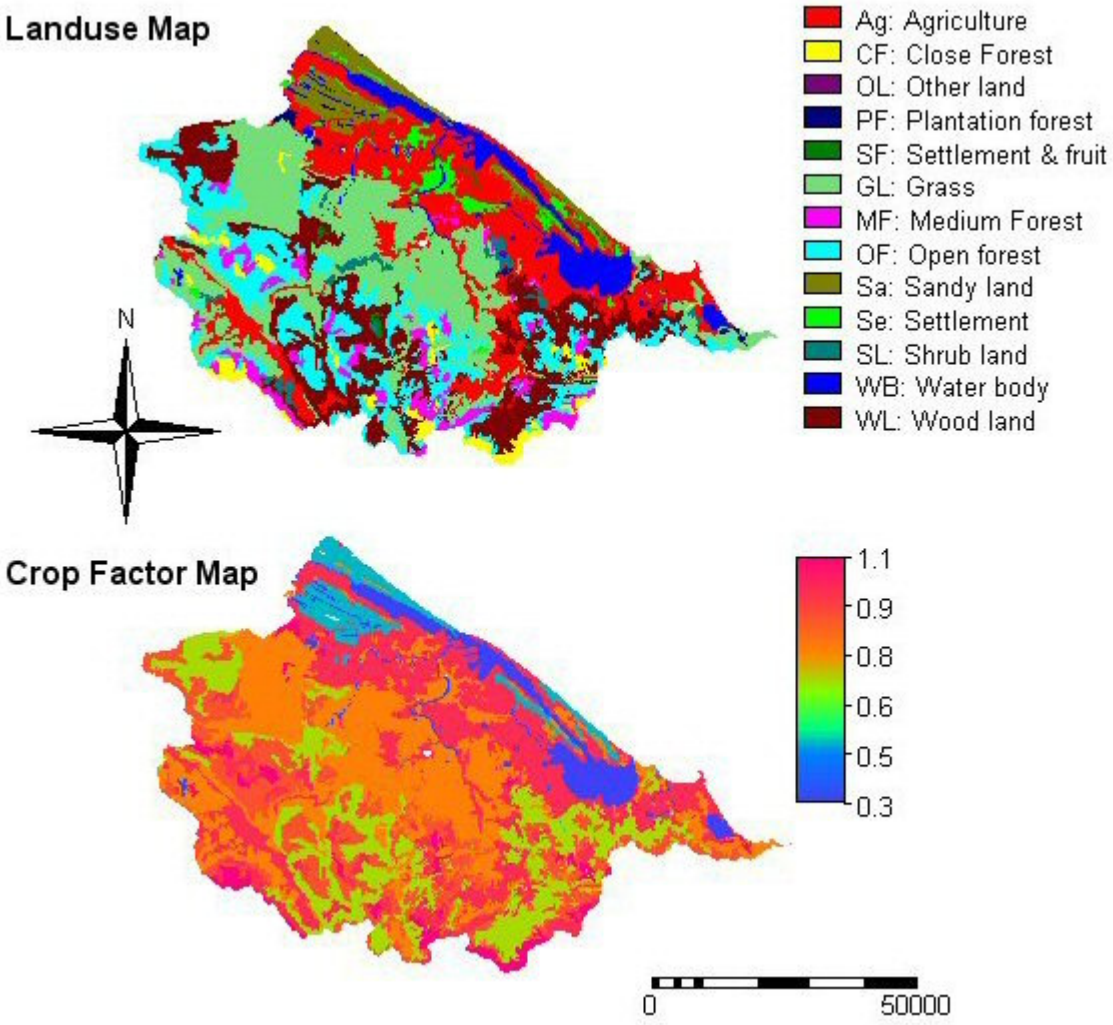

Landuse classes and the Crop Factor indexes (According to Deursen and Kwadijk, 1994)

Class	*Crop factor*
Agriculture	1
Close Forest	1.1
Grass	0.8
Medium Forest	1
Open forest	0.9
Settlement	0.8
Wood land	0.7
Sandy land	0.5
Plantation forest	1.1
Other land	0.5
Shrub land	0.8
Settlement & fruit	0.8

Figure 15. Landuse map, derived Crop Factor map and table with the factor values.

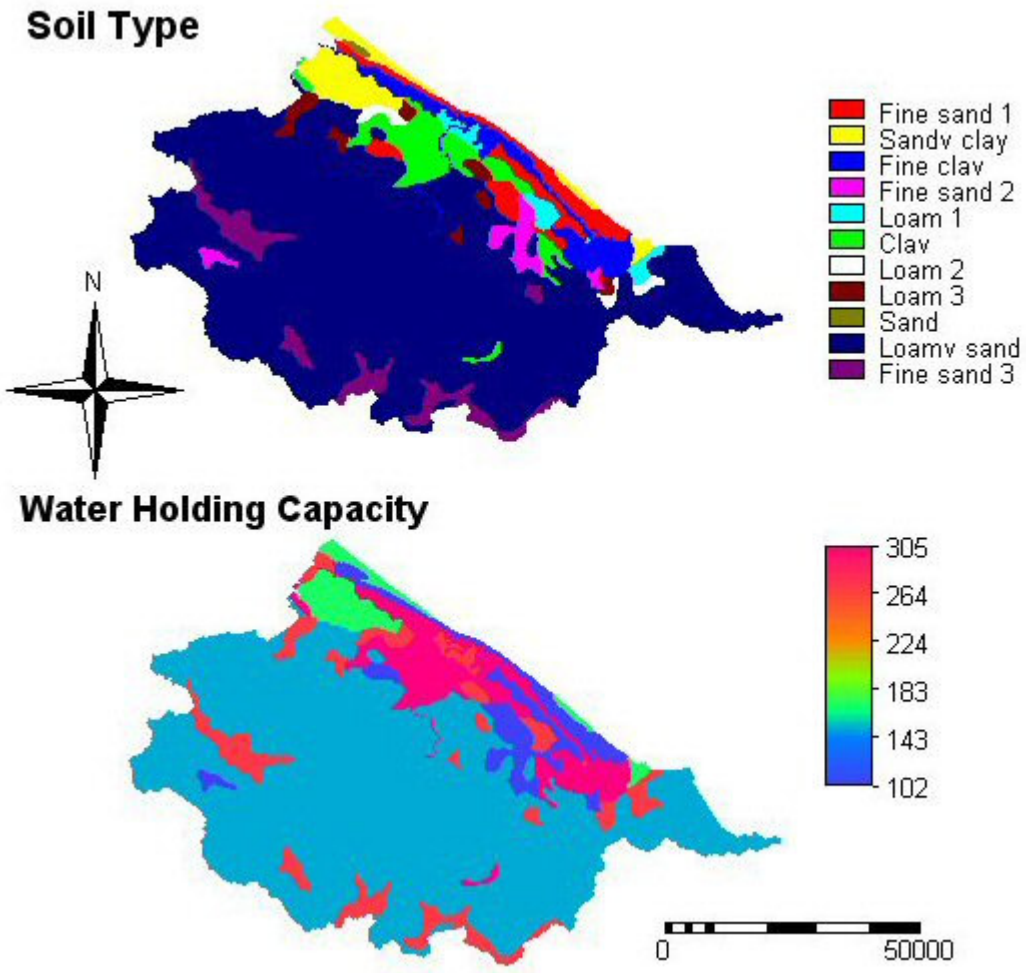

Soil Type classes and the Water Holding values (According to Deursen and Kwadijk, 1994)

Class	*Whold*
Fine sand 1	102
Sandy clay	170
Fine clay	305
Fine sand 2	102
Loam 1	270
Clay	305
Loam 2	270
Loam 3	270
Sand	102
Loamy sand	150
Fine sand 3	270

Figure 16. Soil Type map, derived Water Holding Capacity map and Table with values.

3.4. Running the model

Running the STREAM model is the next step once all the input maps are obtained. To run STREAM the following files are needed:

- Daily (32) precipitation (PRE)
- Daily (32) temperature (TMP)
- Daily (32) daylight (day)
- Initial map for APWL
- Initial map for GW
- Initial map for SOILSTOR
- Map for A
- Map for HEAT
- Map for C
- Map for Covermap
- Map for MASK
- Map for WHOLDN

To run the model, the script is also needed. The calculation script, based in BLAISE language, is detailed in the Appendix 1.

To see values of specific points (especially useful for creating hydrographs) a discharge file also has to be created. This is a simple text file named Qout3.dis, with the following structure:

243 248 Thuong Nhat

The first number is the row, the second the column. To look up these coordinates we have to make use of IDRISI. It is best to first run STREAM without the Qout3.dis (and thus also placing a # before the scriptlines refering to Qout3.dis (i.e. `timeout(DISQSEC, %DischargePoints, %OutputDirectory)`. The row and columns presented in IDRISI aren't however the numbers that should be entered into the file. It should be added one to the number of the row and column (In Idrisi: R 242, C 247 -> Qout3.dis: R 243, C 248).

3.5. Model Efficiency Test

The performance of the model was tested using a model efficiency coefficient. The model efficiency coefficient R2 from Nash and Sutcliffe (1970) where 1 represents the perfect match and smaller values represents worse matches, is calculate using the equation:

$$R^2 = \frac{F_0^{\,2} - F^{\,2}}{F_0^{\,2}} \tag{5}$$

The initial variance $F_0^{\,2}$ in Equation 1 is calculated using the following equation:

$$F_0^{\,2} = \sum (q_i - \overline{q})^2 \tag{6}$$

where $\overline{q}$ is the mean observed runoff and q_i the observed runoff at time step i. The index of disagreement is calculated using the following equation:

$$F^2 = \sum (q_i^{'} - q_i)^2 \quad (7)$$

where $q_i^{'}$ is the modelled runoff value and q_i is the observed runoff value at time step i. The two R^2 values will be compared and the model with the best performance will be selected.

3.6. Reservoir Model

The simplest reservoir model (Free draining reservoir) considers a semi-closed space, an input and an output of water, governed by the rates (normally $m^3\ s^{-1}$) of charge and discharge. If during a flooding period the water coming into a small-scale area is accumulated because the output rate of the water is less than the input, means that this area can be considered like a natural reservoir. Taken in consideration this assumption and the fact that the coastal plain of the Hue province could accumulate the water during the 1999 flooding event, we can considerate this area like a natural reservoir with an input of water from the rainfall in the mountains and the output to the sea. For practical reasons, the processes of losses (evapotranspiration and infiltration) in the flood plain and some gains (groundwater inflow) are assumed not to have significant effect compared with the massive amount of runoff and rainfall water stored.

The free draining reservoir in its conceptual definition is a storage augmented by inflow and depleted by outflow through its opening (Figure 17). The parameters to estimate in this model will be q the outflow; V that is the reservoir storage or the input.

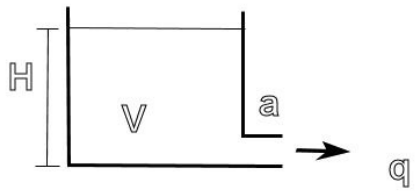

Where there is not input, i.e. only outflow is considered, the well known linear reservoir formula is obtained:

$$V_t = V_0 . e^{-\alpha} \quad (8)$$

Figure 17. Free draining linear reservoir

where *Vt* is the Volume in the time step *t*, *Vo* is the volume in the time step 0 and α is the reservoir outflow recession constant (Wolski 1999). Non linear reservoir models were not considered because of the lack of enough data.

To see if the flooding area could behave like a reservoir, three cross-sections were analyzed in the DEM to see the variation of the altitude with the distance. The

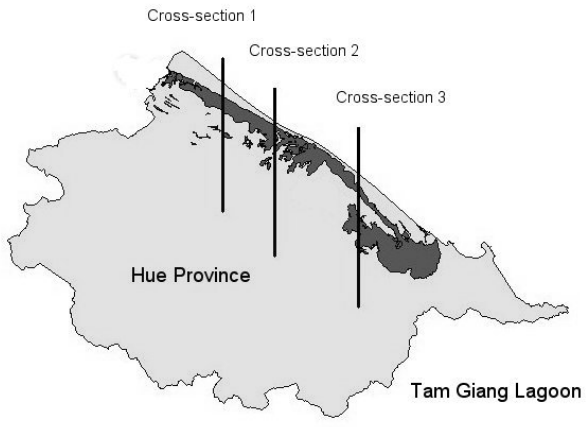

Figure 18. Cross-sections traced on the DEM.

location of the three cross-sections is shown in the Figure 18. The objective of this map calculation was to test effectively if the flood plain is semi closed area.

The resulting profiles of the variation of the altitude according to the distance are shown in the Figure 19. In the three profiles it is seen that the dunes in the seaside act as a barrier turning the system of coastal lagoons semi-isolated. In the section 1 the dunes altitude reach the 20 m over the sea level and there are approximately 20 km of flood plain below this height. The drastic change from 10 to 140 m over the sea level in less than 1 km determines the limit of this zone. In the case of the Section 2, the same pattern is seen with very variable height, determined by the several small lagoons occurring in this area. In this section there is also the presence of the Hue city. The Section 3 presents a similar pattern than the observed in the section 1.

(a)

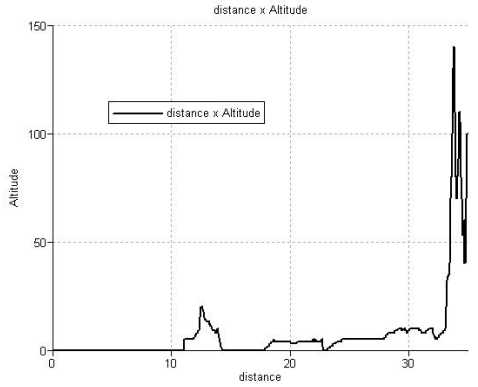

(b)

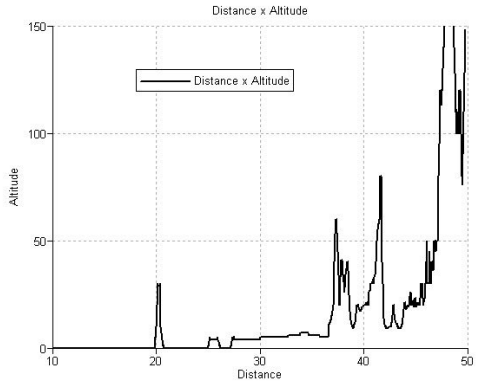

(c)

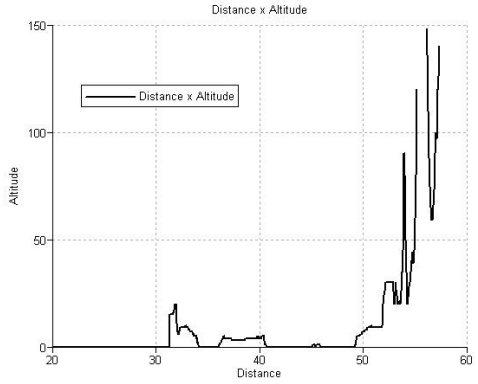

Figure 19. Altitude profile of the three Cross-sections in the DEM: (a) Cross section 1, (b) Cross section 2 and (c) Cross section 3.

After these results it is expected that the water coming from the mountains as a runoff will be accumulated and the water level at the flood plain would be approximately horizontal. This last approach will be tested with the real extension of the flood at 6th November Radarsat image and check the altitude of the border of this extension with the help of the DEM by crossing these two maps (Section 3.8).

Finding out the volumes in different time steps should be enough to get a reservoir depletion curve and estimate the depletion constant α. The actual volumes will be estimated by the use of the RADARSAT imagery.

A simple Inflow – Storage – Outflow relationship will be found with the Inflow volume amounts obtained from the model and the daily depletion of the volume stored in the flooding area extracted from the RADARSAT images. The objective of this calculation will be the determination of the flow outside the reservoir model and the time of permanence inside the flood plain. Obviously, to have a relationship between incoming and outgoing volumes through the flooding area, a horizontal water level of the inundation is assumed.

3.7. Flooding area extraction from RADARSAT images

The application of Synthetic Aperture Radar imagery to assess the flooding extension has been well studied during the last years (Bates, Horritt et al. 1997; Nico, Pappalepore et al. 2000; Horritt and Mason 2001). This technique is based in the fact that the water has much less scattering registered by the sensor when the signal hits the liquid surface compared to the soil surface. This effect is more related to the roughness of the surface that determines the amount of the scattering. The water surface is in the most of the cases plane and is seen dark in the RADARSAT images while the land surface is shown brighter.

The goal of the flood area extraction is to determine the threshold pixel value that determines the limit between water and land. This can be possible through a very detailed analysis of the water – land interface and stretching techniques.

Three SAR - RADARSAT images corresponding to 6th, 10th and 15th November were kindly provided by Dr. T. D. Lan from the Haiphong Institute of Oceanography. These three images were imported with the help of ERDAS IMAGINE 8.6 that permits to read directly RADARSAT CEOS file formats. Then these three images were imported in ILWIS 3.2 to perform the flooding area extraction.

3.8. Water level of the flooding area

The flooding level was calculated with the help of the RADARSAT image corresponding to 6th November. The objective of this analysis was to find out if the water level has a horizontal behaviour. This assumption was considered in the Section 3.6 but need to be tested. One way to obtain this information was by using the actual extension of the flooding area obtained in the previous section and extracts the border limiting the inundation. This border map was crossed with the DEM to have an idea of the altitude of this line.

Once this map was obtained, it was seen that there was not a trend in the geographical distribution of the values. There were not higher or lower values separately distributed but were disseminated indiscriminately. In the frequencies chart the most common altitude values in the border ranged between 4 and 5 m. The graph with the frequencies of the altitude values is shown in the Figure 20.

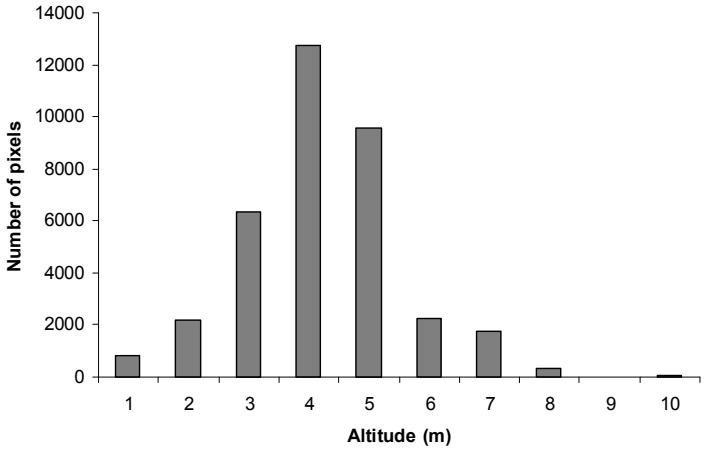

Figure 20. Graph with altitude frequencies of the flooding area border.

4. Results

In this chapter the outputs of the STREAM model will be shown. The comparison between the results with rainfall data collected in the ground and the TRMM rainfall estimation will also be shown. A statistical analysis will be performed in order to select between the two outputs the most reliable rainfall estimation to calculate the total volume of water coming into to the coastal plain during the typhoon days (between 1 and 6 November) and estimate the extension of the areas of flooding according to discharges obtained. At the end a comparison between this result and real flooding extensions obtained from Radarsat imagery will be made.

4.1. Stream Output

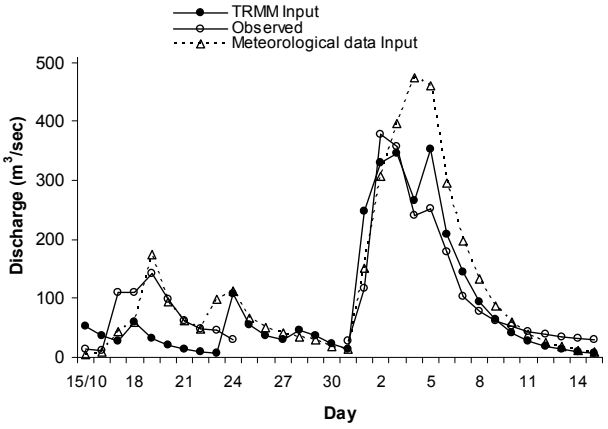

Figure 21. Actual and modeled discharges at Thuong Nhat station

The discharges Ta Trach River at the station of Thuong Nhat and the output from the STREAM model at this point (both meteorological interpolated data and the TRMM) were compared to see how well they fit. In the Figure 21, the three results are compared. In the graph is observed that in the first days the discharges obtained from the rainfall interpolation from the meteorological stations fits better the discharges collected in the ground than the TRMM rainfall estimations. But after then and especially during the flooding period the contrary is observed and the TRMM estimations fits better the actual discharges. The interpolation from the meteorological stations overestimates the discharges during this period especially the peak at 2nd November. For that reason the TRMM data was chosen for the total volume calculation and flood area estimation.

Table 6. Calculated discharges at the source points ($m^3 s^{-1}$)

Day	Pt 1	Pt 2	Pt 3	Pt 4	Pt 5
1	546	1732	3603	270	278
2	778	3065	5940	432	433
3	819	2750	5157	373	412
4	648	2260	4021	284	272
5	643	2435	4279	278	332
6	414	1596	3456	217	206

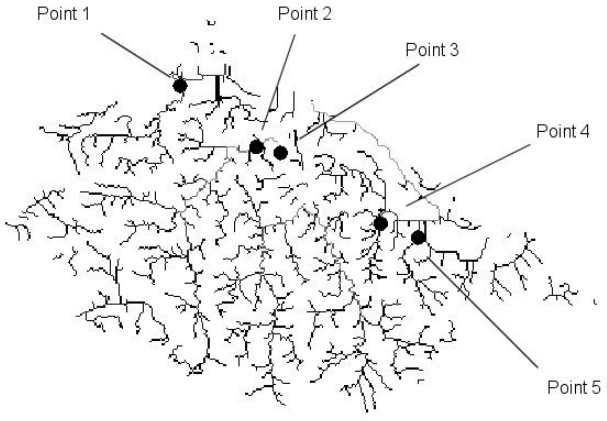

Figure 22. Selected points for discharge calculation

In the first run of the model a map of discharges was obtained as a part of the results from the Stream Model. With this discharge map (Figure 22) the most important sources of runoff to the coastal plain were established and selected to show the discharge at this points in the next iteration. In this way, the total discharge during the 6 days of flooding was calculated. The discharge in m^3/sec of each point at their geographical positions obtained from the STREAM model is detailed in the Table 6.

4.2. Volume estimation

The discharges calculated in daily basis are shown n the Table 7.

Table 7. Daily volume of water discharged into the flooded area (Mm^3)

Day	Point 1	Point 2	Point 3	Point 4	Point 5
1/11	47.1	149.7	311.3	23.3	24.0
2	67.2	264.8	513.2	37.4	37.4
3	70.7	237.6	445.6	32.2	35.6
4	56.0	195.3	347.4	24.5	23.5
5	55.6	210.4	369.7	24.1	28.7
6	35.8	137.9	298.6	18.7	17.8
Total	**332.4**	**1195.6**	**2285.8**	**160.2**	**167.0**

The total amount of water coming into the flooding area is 4 140 x 10^6 m^3 during the 6 days of flooding. That means that approximately 4 000 millions of cubic meters were accumulated in the coastal plain without considering the amount of water coming from direct rain over this area. To estimate the direct rainfall the TRMM raster images were used. The total volume of water calculated is shown in the Table 8

Table 8. Total daily volume of direct rainfall over the flooding area

Day	Volume (Mm^3)
1/11	242.8
2	225.5
3	214.7
4	32.5
5	67.4
6	90.5
Total	**873.4**

The total volume of water would be the sum of these two components: the rainfall that fell down over the flood area, and the discharges coming from the mountains runoff. This volume is 5 014 Mm^3 during the 6 days of flooding, that means that approximately 5 thousands million of cubic meters were accumulated in the coastal plain of TT Hue.

4.3. Flood extension simulation

Once the total volume of water is obtained, the calculation of the extension of the flooding area can be calculated. A map calculation was made using ILWIS on the DEM to find the extension that would be

reached by this volume with several scenarios of flooding. The results of this DEM inundation are detailed in the Table 9. This table shows the water level of the flood scenarios and their corresponding area and volume reached by each case. The water level is considered to be measured from the 0 meters in the DEM.

Table 9. Results of the DEM inundation with different scenarios of flooding

Water level (m)	Area (km^2)	Volume (Mm^3)
0.5	274	**95**
1	359	**262**
1.5	389	**452**
2	409	**652**
2.5	425	**862**
3	459	**1084**
3.5	502	**1326**
4	561	**1594**
4.5	633	**1896**
5	744	**2243**
5.5	867	**2665**
6	903	**3110**
6.5	932	**3570**
7	961	**4045**
7.5	990	**4534**
8	1019	**5038**
8.5	1044	**5555**
9	1073	**6085**
9.5	1123	**6635**
10	1210	**7220**

If we compare the results of the DEM inundation with the volume calculated in the section 5.2 we will realize that the most likely scenario of flooding is the one that corresponds to the 8 m of water level. The volume reached by this scenario is approximately 5 thousands million cubic meters in both cases.

This would be the possible scenario if the entire amount of water were accumulated in the coastal plain. Anyway, this is not a realistic approach due to the fact that there is a connection between the coastal lagoon and the sea, *i.e.* where there is an output.

A comparison will be made between this result and the actual area estimations from Radarsat images.

4.4. RADARSAT Flooding area anaysis

For the next step in the analysis, the extension of the flooding area resulting from the radar image processing was calculated and an estimation of the volume estimated. The results of flooding area extraction are shown in the Figure 23

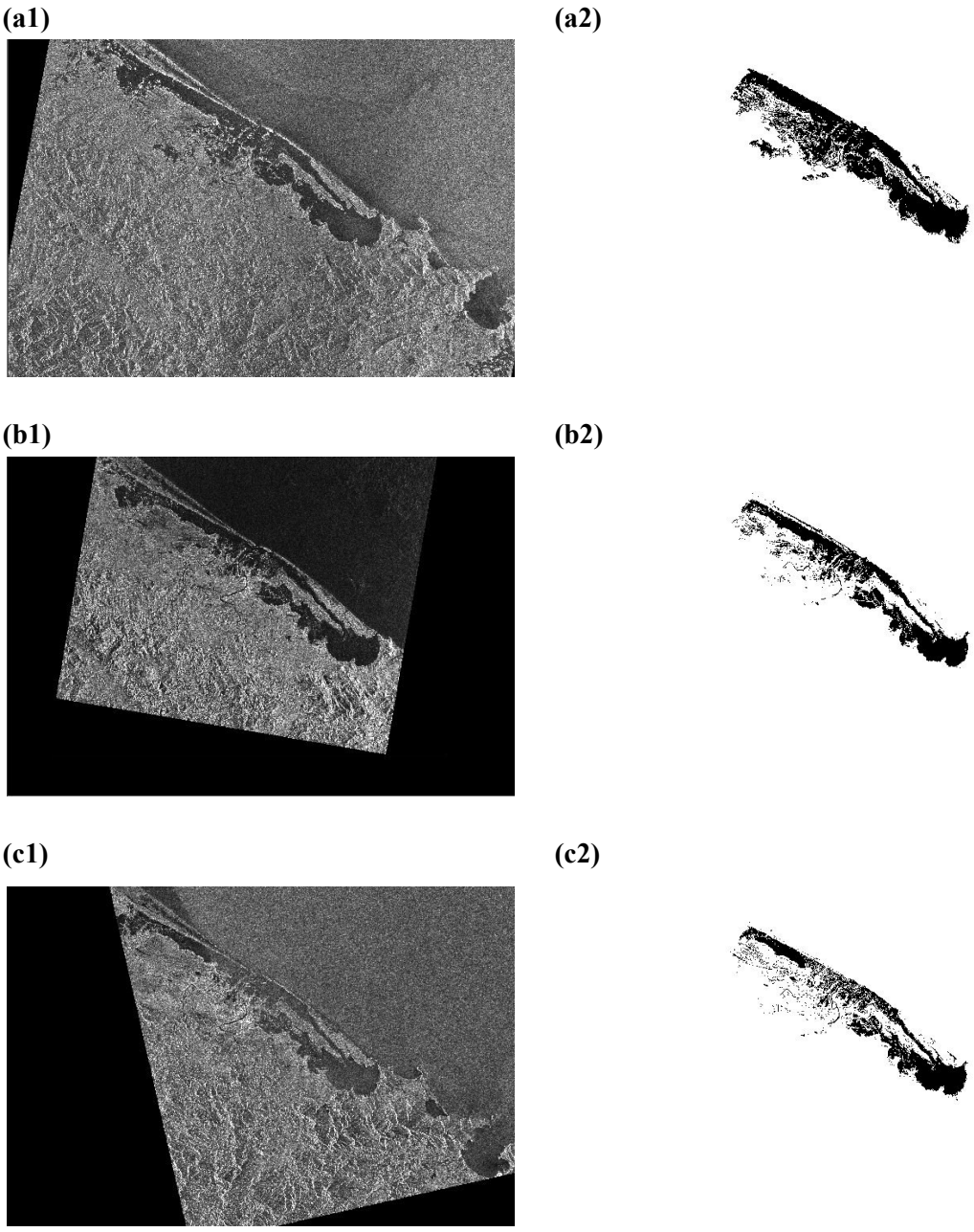

Figure 23. Radarsat images and their corresponded extracted flooding area map: (a) 06/11/99, (b) 10/11/99 and (c) 15/11/99.

In the Figure 23a, b and c the Radarsat images are observed with the flooding extension obtained so far. To estimate the total flooded area in each image a map calculation has been made in which the pixel size (30 m) is multiplied by the number of pixels. The results of the three area estimation and the calculated volume are shown in the Table 10. The volume was extrapolated from the relationship between the Area and Volume values in the Table 9

Table 10. Estimated flooded area and volume from the Radarsat images

Date	Area (x 10^6 m^2)	Estimated volume (Mm^3)
6/11	686.5	2059.4
10/11	451.0	1064.4
15/11	424.8	858.0

With these values an exponential relationship was fitted to the data. The results of the plot are shown in the Figure 24.

With the exponential regression fit, the outflow rate parameter could be estimated as being 0.095. Assuming that this curve is the depletion trend of the volume stored in the flooding plain, a simple Inflow – Storage – Outflow model based in a Reservoir Model could be fitted. To run this model the following parameters must be calculated:

Input volume: (*Vin*) The input parameter used was the Inflow volume already calculated with Stream that is the daily sum of the volumes estimated in the 5 points during the whole study period (32 days), summed to the direct rainfall over the flooding area calculated in the section 4.2.

Output volume: (*Vout*) The output volume will be a function of the stored volume, the time of residence inside the reservoir and the minimum daily volume of discharge out of the flooding area. The relationship was defined using the following conditional expression:

$$V_{out} = iff\left(V_{stor} \le MDV, V_{stor}, iff\left[(V_{stor} - MDV) \div RT\right] \le MDV, MDV, \left[(V_{stor} - MDV) \div RT\right]\right) \quad (9)$$

where:

MDV = Minimum Daily Volume of Discharge
RT = Residence Time – *1/e* value

Stored Volume: (V_{stor}) is defined like the sum of the previous V_{in} and V_{stor} minus the V_{out}. To calculate this, an initial value should be entered. An amount of 100 Mm^3 of initial volume was considered taken in account the 0 order magnitude of the incoming flow. (In the order of 100 Mm^3 approximately).

The objective of this calculation was to fit the exponential relationship of the Radarsat volumes depletion curve to a depletion curve of the volume stored (V_{stor}) and in this way obtain the relation Inflow – Storage – Outflow as is shown in the Figure 24. In this plot the estimated stored and the Radarsat estimated volumes in the flood plain have the same depletion curve

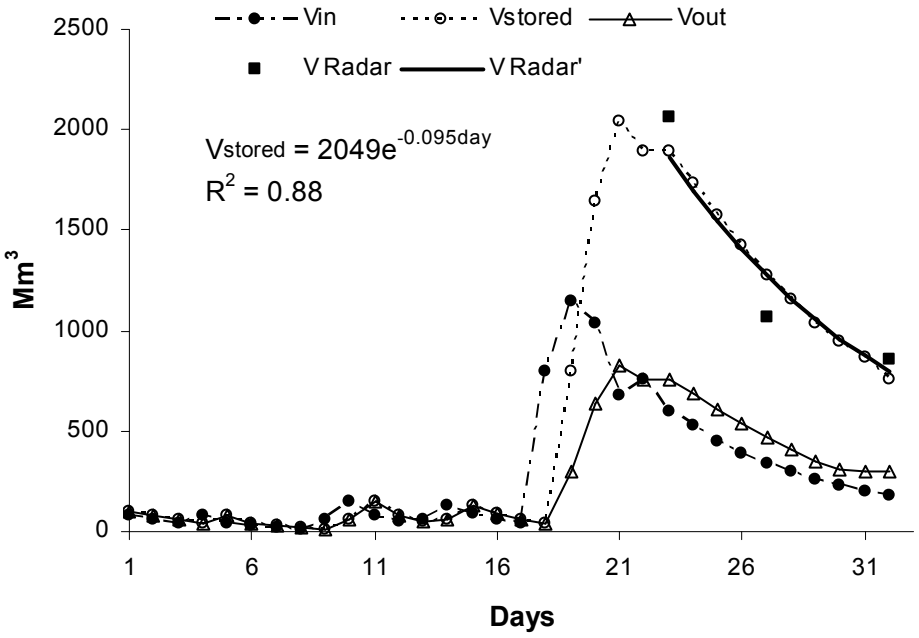

Figure 24. Plot of the reservoir model results, V_{in}: Volume of the inflow, V_{stored}: Calculated volume stored, V_{out}: Volume of the outflow, V_{Radar}: Volume extracted from the Radarsat images, V_{radar}': Fitted exponential curve from V_{Radar}.

The results of this calculation are shown in the Table 11

Table 11. Results of the Reservoir model calculations. The flooding period is shown in bold numbers

Nday	Vin	Vstored	Vout	Water level
1	77.7	100.0	100.0	0.44
2	57.3	77.7	77.7	0.35
3	37.8	57.3	57.3	0.26
4	76.3	37.8	37.8	0.17
5	44.6	76.3	76.3	0.34
6	29.4	44.6	44.6	0.20
7	19.6	29.4	29.4	0.14
8	13.0	19.6	19.6	0.09
9	57.6	13.0	13.0	0.06
10	151.4	57.6	57.6	0.26
11	81.5	151.4	151.4	0.64
12	54.2	81.5	81.5	0.37
13	57.7	54.2	54.2	0.25
14	126.2	57.7	57.7	0.26
15	93.4	126.2	126.2	0.55
16	58.2	93.4	93.4	0.42
17	38.8	58.2	58.2	0.27
18	797.0	38.8	38.8	0.18
19	1144.0	797.0	300.0	2.43
20	1037.0	1641.0	638.6	3.99
21	678.5	2039.4	828.3	4.60
22	756.4	1889.6	757.0	4.38
23	600.5	1889.1	756.7	4.38
24	525.5	1732.9	682.3	4.14
25	452.5	1576.0	607.6	3.89
26	390.7	1420.8	533.7	3.63
27	338.4	1277.8	465.6	3.38
28	294.1	1150.5	405.0	3.14
29	256.6	1039.6	352.2	2.93
30	224.9	944.1	306.7	2.74
31	198.1	862.3	300.0	2.57
32	175.3	760.3	300.0	2.35

Where V_{in} is the inflow volume obtained from the STREAM results, $(V_{stor})_i$ is:

$$(V_{stor})_i = (V_{ini})_{i-1} + (V_{stor})_{i-1} + (V_{stor})_{i-1}$$

An initial stored volume of 100 Mm^3 was considered, although this initial input does not have a significant effect in the next calculations. V_{out} is defined by the condition shown before in this section (Equation 9) with the difference that the *MDV* and *RT* were replaced by the best values to fit the exponential depletion curve from the Radarsat analysis:

$$V_{out} = iff\,(V_{stor} \le 300, V_{stor}, iff\left[(V_{stor} - 300) \div 2.1\right] \le 300, 300, \left[(V_{stor} - 300) \div 2.1\right]$$

where

MDV = 300 Mm^3, and
TM = 2.1 days

This means that the time of permanence of the water in the flooding plain is approximately 2 days with a base outflow of 300 Mm^3 per day. The water level was based in the map calculation outputs with the DEM (Table 9). The function that explains the variation of the water level with the volume is:

$$WL = \frac{-199.6 + \sqrt{199.6^2 - 4 \times 52.9} \times 1.4 - V_{stor}}{2 \times 52.9} \quad (10)$$

This is the solved equation of the polynomial relationship between the volume stored in the flood plain and the water level of the flood. It is observed that the volume calculated with this function is coincident with the height of the water level estimated in the Section 3.8. Both results ranged between 4 and 5 m.

Is also shown in the table the onset of the flooding at the day 18 (1st November) and the response in the stored volume has a delay with the peak of this volume at the day 21.

5. Discussion and Conclusion

In tropical regions, floods are one of the most important natural disasters as they cause losses of human lives when populated areas are inundated. Damages in crop fields, agricultural lands as well as roads and communication network cause great economic losses that these countries, the most of them part of the third world, can not afford. These disasters normally are followed by epidemic diseases blooms due to the lack of fresh water and food combined with a destroyed infrastructure, making it more difficult to distribute humanitarian help. The knowledge of techniques that could be used in the implementation of appropriate planning, as a key tool to improve flood management, is needed. One of these tools is the delimitation of flooded areas though the analysis of Remote Sensing data that would permit by mean of several techniques, to map in a detailed way, actual extension of the inundated areas.

But the coupling of Remote Sensing data with GIS based models, which can provide spatial and temporal data would help to represent natural hydrological processes more accurately. This synergy would also give dynamic ways of understanding phenomena in the environment. This research is aimed to be one example of what the coupling between Remote sensed imagery (TRMM and RADARSAT images) and GIS tools like the STREAM model can do in the understanding of a disaster event like the flooding in Hue City in November 1999.

In this study, the use of satellite based rainfall estimations has been proved to be useful in extreme storm events like the typhoon of November 1999. Although the rainfall estimation, tried in this study, in the whole catchment area by rain gauge data interpolation could not be a realistic approach taken in consideration the few meteorological stations in the Hue province and the high level of uncertainty related to its spatial distribution, the discharge obtained in the modeling with this data fits well to the observed values (Thuong Nhat station) during the days previous to the flooding event. The contrary is observed during the flooding period when the discharges obtained with the modeling with the TRMM rainfall estimations fit the observed values better.

The differences between the discharges obtained with the rain gauge data interpolation and the TRMM estimations observed are high during normal conditions. The spatial distribution and the small number of the rain gauge stations could be the principal reason. The TRMM data is better at estimating the spatial distribution of the rainfall instead of the temporal resolution, which is the advantage of the more accurate rain gauge data. Rain gauges measure more or less continuously in time but cover very little of the area, whereas satellite observations are more widely spaced in time. This is the case of the TRMM satellite; because of its closeness to the earth the coverage is not frequent. The period of study and the time steps are also a very important factor to take in consideration in the discussion of the results. TRMM 2A12 products are based in rainfall rates of mm/hour, but the pass time is in the best case 1 per day and there are even days when there are no passes at all. The products that cover daily estimations (Level 3 products) have spatial resolution of more than 1° x 1° degree. Logically this resolution is insufficient for small and medium catchment areas, like the Perfume River of less than 1 squared degree.

The possibility of calibration of the hourly TRMM data to daily estimations of rainfall is suggested in this study. However the linear function used in the hourly TRMM and the daily ground collected rainfall is not accurate. One possibility for future studies in this area could be the adjustment or calibration of the hourly data to daily by mean of the R^2 or σ analysis with a longer time series or with bigger grid sizes in the order of 1° x 1° degree or more (Bell 2001). According to Kummerow (2001), sparse rain gauges in a number of grid boxes contribute to an additional source of uncertainty. The possibility of another function instead of the linear is also suggested.

One of the most common methods of comparing satellite estimates of rainfall with ground-based observations and with other satellite estimates is to test the agreement of averages over a spatial domain, such as a grid box on a map, averaged over a sufficiently long time period that the averages are stable enough for the comparison to be informative. Even if the remote sensing techniques are perfectly accurate, such averages will contain sampling errors, because the systems are not measuring rainfall everywhere in the area at every moment. Although averages from two different systems may disagree because of inherent errors in the measurement methods, they will almost certainly disagree because they contain different sampling errors (Bell 2001).

However, the results obtained so far with the TRMM data are promising and its use could be carried out in areas with low and sparse number of rain gauges. Its use is especially suggested to study strong tropical rainfall events like cyclones and the hydrological processes accompanying those, like floodings and assessment of their disastrous consequences.

The documentation about the uses of the TRMM data to assess tropical cyclones and estimate rainfall rates for meteorological forecasts is well known. The webpage of the TRMM http://trmm.gsfc.nasa.gov offers information of tropical cyclones and other extreme events like storms and floodings all around the tropical area of the world. This service also provides location of potential floods due to heavy rain accumulation in 24, 72 and 168 hours based in thresholds (35 mm, 100 mm and 200 mm respectively).

The other Remote Sensing approach tested in this study was the use of set of SAR – RADARSAT images to estimate the flooded area and from this the volume of water accumulated. In the last years the use of Radar imagery has been highlighted because of its all-weather performance and day and night capabilities, very useful during periods of flooding that normally shows cloudy conditions (Schultz and Engman 2000). Although the flood extension extraction from SAR images has been well documented, this technique is still under study (Wang, Hess et al. 1995; Horritt and Mason 2001). To define simply a threshold to differentiate flooded of non-flooded areas is after all a subjective technique. The best approach to be adopted to define flooded areas is to compare two different SAR sets of the same region: one taken before and the other immediately after the flood event and detect the water filled zones by looking at the decreased backscatter signal in a pixel by pixel basis (Nico, Pappalepore et al. 2000). For this study the flood area maps that were obtained from the Radar imagery were based on the extraction of the low backscattered signal areas that were supposed to be areas covered by water. No comparison could be made with stages before the flooding event due to the lack of SAR images in the period pre-flooding. Nevertheless a study of comparative scattering values can be made in future studies to corroborate the results obtained here if images from dry periods are available.

The principal obstacle during the flooding area extraction was to find the correct threshold value between the water – land boundary. This technique is still under testing because of the subjectivity involved in the process. Some studies suggested the use of the differential coherence between SAR images of the same area to eliminate possible sampling errors in the threshold selection and give to the process a more numeric approach (Nico, Pappalepore et al. 2000).

The situation is, however, more complicated as the water surface may be roughened by wind or broken by protruding vegetation, the image may be degraded by speckle and the sideways-looking radar system can produce complex returns from topography that may introduce distortion into the images. To date, much of the literature on delineating flood boundaries using SAR adopts a qualitative approach. In spite of this, SAR data processed with a simple density stretching, slicing and threshold technique provided a better identification of the flooded area (85% correct) compared with Landsat (64% correct) when compared with an aerial photograph control (Bates, Horritt et al. 1997). The presence of aquatic vegetation, mangrove areas and aquaculture infrastructure should be taken in consideration as it was observed during the visit to the study area during the fieldwork. The presence of urban and human settlement areas should be also assessed especially in the surrounding areas of the principal rivers where high reflectance in the RADARSAT images are expected even if they are inundated with water because of houses roofs rising over the water level. It was observed in the fieldwork that there is a high occurrence of settlements nearby the border of rivers because of the access to the water.

The STREAM model was proved to perform well to test the discharges for the reconstruction of the flooding event. The trends shown in the results seem to be in accordance with the observations made. The use of lower resolution data (300 m of pixel size) looks appropriate to be applied in the flooding modeling, although the use of a more detailed DEM with more vertical resolution, maybe with 1 m in the first 10 m altitude instead of the 2.5 m used in this study, would be useful for the flooding limit delineation using simple map calculation using the DEM.

Despite of the realistic results in the map calculation with DEM and the respective area and volume calculation, there is a lack of information about water levels measuring within the flooding area that could be useful in the calibration of the model in the height estimations with the DEM (Table 9). Water level measures were available in the Kim Long station showing a peak of water level in the Perfume River between the 2nd and 3rd November of 5 meters but a recession curve much more pronounced during the next days. This could be explained because this station is located near the border of the flooding area close to the city of Hue and a more pronounced depletion curve is expected. Water levels measuring data of the Tam Giang lagoon would be useful in the flooding area estimation using the DEM inundation that was proved to be effective in the calculation of the area and volume of the flood and a helpful tool in the modeling of these events.

6. References

Aerts, J. C. J. H. and L. M. Bouwer (2002). STREAM Perfume - Calibration and Validation for the wider Perfume River Basin in Vietnam, Institute for Environmental Studies (IVM), Vrije Universiteit, Amsterdam**:** 35.

Aerts, J. C. J. H., M. Kriek, et al. (1999). "STREAM (Spatial Toools for River Basin and Environment and Analysis of Management Options): "Set up Requirements"." Physics and Chemistry of The Earth **24**(6): 591-595.

Bates, P. D., M. S. Horritt, et al. (1997). "Integrationg Remote Sensing Observations of Flood Hydrology and Hydraulic Modelling." Hydrological Processes **11**: 1777-1795.

Bell, T. L. K., Prasun K. and Kummerow, Christian D. (2001). "Sampling Errors of SSM/I and TRMM Rainfall Averages:Comparison with Error Estimates from Surface Data and a Simple Model." Journal of Applied Meteorology **40**.

Deursen, W. P. A. and J. C. J. van Kwadijk (1994). "The impact of climate change on the water balance of the Ganges-Brahmaputra and Yangtze basin." RA/94-160.

Horritt, M. S. and D. C. Mason (2001). "Flood boundary delination from Synthetic Aperture Radar imagery using a statistical active contour model." International Journal of Remote Sensing **22**(13): 2489-2507.

Hou, A. Y., S. Q. Zhang, et al. (2001). "Improving Global Analysis and Short-Range Forecast Using Rainfall and Moisture Observations Derived from TRMM and SSM/I Passive Microwave Sensors." Bulletin of the American Meteorological Society **82**(4).

Kummerow, C., Y. Hong, et al. (2001). "The Evolution of the Goddard Profiling Algorithm (GPROF) for Rainfall Estimation from Passive Microwave Sensors." Journal of Applied Meteorology **40**: 1801-1820.

Kummerow, C., J. Simpsom, et al. (2000). "The Status of the Tropical Rainfall Measuring Mission (TRMM) after Two Years in Orbit." Journal of Applied Meteorology **39**: 1965-1982.

Levizzani, V. and R. Amorati (2002). A Review of Satellite-based Rainfall Estimation Methods. Bologna, Italy, Consiglio Nazionale delle Ricerche Istituto di Scienze dell'Atmosfera e del Clima**:** 66.

Menzel, W. P. and J. F. W. Purdom (1994). "Introducing GOES-I: The First of a New Generation of Geostationary Operational Environmental Satellites." Bulletin of the American Meteorological Society **75**: 757-782.

Nash, J. E. and J. V. Sutcliffe (1970). "River flow forecasting through conceptual models part. I - A discussion of principles." Journal of Hydrology **10**(3): 282-290.

Nico, G., M. Pappalepore, et al. (2000). "Comparison of SAR amplitude vs. coherence flood detection methods - a GIS application." International Journal of Remote Sensing **21**(8): 1619-1631.

Phap, T. T. and L. T. N. Thuan (2002). Tam Giang Lagoon aquatic systems health assessment. Primary Aquatic Animal Health Care in Rural, Small-scale, Aquaculture Development. I. H. MacRae, FAO Fish. Tech. Pap. **406**.

Rui, H., B. Teng, et al. (2002). "Statistics of TRMM Data Archive and Distribution at the GES DAAC."

Schmetz, J., P. Pili, et al. (2002). "An Introduction to Meteosat Second Generation (MSG)." Bulletin of the American Meteorological Society **83**(7): 977-992.

Schultz, G. A. and E. T. Engman (2000). Remote Sensing in Hydrology and Water Management, Springer.

Simpson, J., C. Kummerow, et al. (1996). "On the Tropical Rainfall Measuring Mission (TRMM)." Meteorology and Atmospheric Physics **60**: 19-36.

Wang, Y., L. L. Hess, et al. (1995). "Understanding the radar backscattering from flooded and non-flooded Amazonian forests: Results from canopy backscatter modeling." Remote Sensing of Environment **54**(3): 324-332.

Wolski, P. (1999). Application of Reservoir Modelling to hydrotopes identified by Remote Sensing. Amsterdam, Vrije Universiteit**:** 192.

7. Appendixes

7.1. Appendix 1: STREAM Model Script

```
# Reading initial values. These values have to be altered iteratively ...
# APWL          the accumulated potential water loss (mm water)
# GW            the groundwater capacity
# SNOW          the initial thickness (mm water) of the snow cover
# SOILSTOR      the soil storage of water
Import(APWL, 'input\init\')
Import(GW, 'input\init\')
#Import(SNOW, 'input\init\')
Import(SOILSTOR, 'input\init\')
Import(COVERmap, 'input\etc\')

# Masking the init input...
APWL  =       APWL / COVERmap
GW    =       GW / COVERmap
#SNOW=        SNOW / COVERmap
SOILSTOR=     SOILSTOR / COVERmap

# Mapping the init...
Export(APWL , %OutputDirectory, 'Input\Palettes\temp.pal')
Export(GW , %OutputDirectory, 'Input\Palettes\prec.pal')
#Export(SNOW , %OutputDirectory, 'Input\Palettes\prec.pal')
Export(SOILSTOR , %OutputDirectory, 'Input\Palettes\temp.pal')

# Reading Etc: Thorntwaite parameters...
# A:            is calculated as follows: A = 0.49 + (0.0179 * HEAT) - (0.000071 * HEAT^2) +
                (0.00000067 *HEAT^3)
# BPGLDD:       is the flow direction of the cell. This map was derived from the DEM
# C:            is a calibration parameter (usually between 3 and 4) to get the discharge peak and low
                flow values right
# COVERmap:     is used to mask the basin (1 (basin) and 0 (outside basin).
# CROPF:        CROP Factor: reflects the effect of crop on PE. This parameter is derived from
                landuse data. This parameter can also be used to calibrate the overall annual runoff
# HEAT:         is calculated as follows: HEAT = sum(TM/5)^1.514 (where Tm is the long term
                monthly average temperature
# MASK:         is used to mask the basin (0 (basin) and -9999 (outside basin).
# WHOLDN:       Water HOLDiNg capacity: reflects the waterholding capacity of the soil (in mm/m)
Import(A, 'input\etc\')
```

```
Import (BPGLDD, 'input\etc\')
Import(C, 'input\etc\')
Import(CROPF, 'input\etc\')
Import(HEAT, 'input\etc\')
Import(MASK, 'input\etc\')
Import(WHOLDN, 'input\etc\')
# Import(CT, 'input\etc\')

# Masking the etc input...
A              =       A / COVERmap
BPGLDD         =       BPGLDD / COVERmap
C              =       C / COVERmap
CROPF=         CROPF / COVERmap
HEAT           =       HEAT / COVERmap
WHOLDN         =       WHOLDN / COVERmap

# Mapping the etc ...
# Export(HEAT , %OutputDirectory, 'Input\Palettes\temp.pal')
# Export(A , %OutputDirectory, 'Input\Palettes\prec.pal')
# Export(CROPF , %OutputDirectory, 'Input\Palettes\prec.pal')
# Export(WHOLDN , %OutputDirectory, 'Input\Palettes\temp.pal')
# Export(MASK , %OutputDirectory, 'Input\Palettes\prec.pal')
# Export(BPGLDD , %OutputDirectory, 'Input\Palettes\prec.pal')
# Export(COVERmap , %OutputDirectory, 'Input\Palettes\prec.pal')

# Reading climate scenario data for each month...
# DAY     is the number of potential sunshine hours per day
# TMP      is the mean monthly temperature (degrees Celsius)
# PRE     is the mean monthly precipitation (mm)
ImportTimer(DAY, %ClimateChange)
ImportTimer(TMP, %ClimateChange)
ImportTimer(PRE, %ClimateChange)

# Masking the etc input...
TMP = TMP / COVERmap
PRE = PRE / COVERmap
DAY = DAY / COVERmap

# Mapping the temperature and precipitation ...
#ExportTimer(TMP, %OutputDirectory, 'Input\Palettes\temp.pal')
#ExportTimer(PRE, %OutputDirectory, 'Input\Palettes\prec.pal')
#ExportTimer(day, %OutputDirectory, 'Input\Palettes\prec.pal')

# end of importing data

# Calculating snow fall, snow cover storage and snow melt (based on TMP)...
```

```
#SNOW1      =      mif(TMP < 0, PRE, 0)
#SNOW       =      SNOW + SNOW1
#MELT=      mif(TMP > 0, 100 * TMP, 0)
#SNOW2      =      min(SNOW, MELT)
#SNOW       =      SNOW - SNOW2
#MELT2      =      SNOW / 24
#SNOW       =      SNOW - MELT2
#PRE        =      PRE + SNOW2 - SNOW1
# ExportTimer(SNOW, %OutputDirectory, 'Input\Palettes\snow.pal')

# Calculate potential evapotranspiration using Thornthwaite.
# The PE is calculated depended on TMP
# The day/12 is necessary because the daylength is given in hours (and should be a factor)
PE     =      16 * (10 * TMP / HEAT) ^ A
EVEN   =      -415.85 + 32.24 * TMP - (0.43 * TMP^2)
PE     =      mif(TMP > 26.5, EVEN, PE)
PE     =      cover(PE, MASK)
PE     =      mif(TMP <= 0, 0, PE)
PE     =      ( PE * (day/12) * CROPF )/30

# Calculate soil storage according to Thornthwaite-Mather ...
PEFF       =      PRE - PE
APWL       =      mif(PEFF < 0, APWL - PEFF, 0)
EVEN       =      SOILSTOR + PRE - PE
SSTOR      =      mif(PEFF > 0, EVEN, WHOLDN * exp(-APWL / WHOLDN))
AE         =      mif(PEFF >= 0, PE, PRE + SOILSTOR - SSTOR)
TOGW       =      mif(PEFF >= 0, max(0, SOILSTOR + PEFF - WHOLDN), 0)
SOILSTOR   =      max(0.000001, SOILSTOR + PRE - AE - TOGW)
APWL       =      mif(SOILSTOR < WHOLDN, WHOLDN * ln(WHOLDN / SOILSTOR), 0)
APWL       =      cover(APWL, MASK)

# Separate direct from delayed runoff (seepage to groundwater)...
RUNOFF     =      0.10 * TOGW
TOGW       =      TOGW - RUNOFF

# Calculate volume of groundwater and baseflow...
GW         =      GW + TOGW
SLOFLO     =      GW / C
GW         =      GW - SLOFLO
ExportTimer(TOGW, %OutputDirectory, 'Input\Palettes\prec.pal')

# Calculate discharge (snow melt + runoff + baseflow),
# and create map of total monthly discharge per cel...
# Normally it should be: DSCHRG      = MELT2 + RUNOFF + SLOFLO
DSCHRG     =      RUNOFF + SLOFLO
```

```
ExportTimer(DSCHRG, %OutputDirectory, 'Input\Palettes\Dis.pal')

# Accumulate discharge from above lying cels (in mm per month) and create discharge graphs...
DISMM          =          accu(BPGLDD, DSCHRG, 'Input\')
timeout(DISmm, %DischargePoints, %OutputDirectory)

# Convert the discharge (from mm per day to discharge in m3 per second).
# 1 cell corresponds to 300 * 300 m = 90000; 1 mm corresponds to 0.001 m -> 90 m3
# 1 day corresponds to 86400 seconds.
DISQSEC        =          DISMM * 90 / 86400
timeout(DISQSEC, %DischargePoints, %OutputDirectory)
ExportTimer(DISQSEC, %OutputDirectory, 'Input\Palettes\dis.pal')

# Stretching discharge maps (only necessary when there are large discharges)...
DISTEMP        =          mif(DISQSEC > 10, DISQSEC , 0)
DISTEMP2       =          mif(DISTEMP < 5000, DISTEMP , 5000)
DISAREA        =          DISTEMP2
ExportTimer(DISAREA, %OutputDirectory, 'Input\Palettes\Dis.pal')

# Calculate aridity index ...
EVEN           =          cover(AE/PE,0)
EVEN           =          EVEN / COVERmap
ARID           =          EVEN
# ExportTimer(ARID , %OutputDirectory, 'Input\Palettes\Arid.pal')

# Summarize (give max, min and average) for Actual evapotranspiration,
# Potential evapotranspiration, groundwater budget, snow cover, etc ...
TSummary(AE, %OutputDirectory)
TSummary(PE, %OutputDirectory)
TSummary(GW, %OutputDirectory)
#TSummary(SNOW, %OutputDirectory)
#TSummary(ARID, %OutputDirectory)
#TSummary(APWL, %OutputDirectory)
#TSummary(TMP, %OutputDirectory)
#TSummary(PRE, %OutputDirectory)
TSummary(TOGW, %OutputDirectory)
#TSummary(SLOFLO, %OutputDirectory)
#TSummary(RUNOFF, %OutputDirectory)
TSummary(SOILSTOR, %OutputDirectory)
#TSummary(PEFF, %OutputDirectory)
#TSummary(DSCHRG, %OutputDirectory)
TSummary(DISQSEC, %OutputDirectory)
#TSummary(DISMM, %OutputDirectory)
#TSummary(DISAREA, %OutputDirectory)

#ExportTimer(PE, %OutputDirectory, 'Input\Palettes\Dis.pal')
```

```
#ExportTimer(PEFF, %OutputDirectory, 'Input\Palettes\Dis.pal')
#ExportTimer(AE, %OutputDirectory, 'Input\Palettes\Dis.pal')
#ExportTimer(TOGW, %OutputDirectory, 'Input\Palettes\Dis.pal')
ExportTimer(SOILSTOR, %OutputDirectory, 'Input\Palettes\Dis.pal')
ExportTimer(APWL, %OutputDirectory, 'Input\Palettes\Dis.pal')
ExportTimer(RUNOFF, %OutputDirectory, 'Input\Palettes\Dis.pal')
#ExportTimer(SLOFLO, %OutputDirectory, 'Input\Palettes\Dis.pal')
ExportTimer(GW, %OutputDirectory, 'Input\Palettes\Dis.pal')
# ************************************************************************

# ...End of iteration.
```

7.2. Appendix 2: Meteorological Data

7.2.1. Rainfall and Discharges

Date	Hour	Rainfall			Discharges		
		Hue mm	A.Luoi mm	Nam Dong mm	Kim Long cm	Phu Oc cm	Thuong Nhat m3/sec
15/10	1	0	0.1	0.8	26	45	14.8
	2	0		0.1	31	46	
	3	0	0.3	0	36	47	
	4	0.1	0.2	0.1	38	51	
	5	0	0.1	0	38	55	
	6		0.1		36	58	
	7				31	60	13.0
	8				28	61	
	9				24	62	
	10				20	62	
	11				17	62	
	12				15	60	
	13			0.4	16	59	12.4
	14		0.3	0.1	22	58	
	15		0.2	0.9	30	57	
	16		0.9	0.1	35	57	
	17		2.1		39	57	
	18		0.5		39	57	
	19				33	56	17.5
	20				27	54	
	21				21	53	
	22				16	51	
	23				11	49	
	24				11	48	11.5
16/10	1				16	47	13.0
	2				22	47	
	3				28	47	
	4	19.0			33	50	
	5	33.0	0.3	0	37	52	
	6	4.4		1.1	35	54	
	7	1.2	0.1	0.3	31	55	9.28
	8	0.4	2.1		26	56	
	9		1.8		23	56	
	10		0.1	0.6	18	55	
	11			10.0	14	53	
	12	0.1		0.3	12	52	
	13	0	0.1	4.1	12	51	8.33
	14		1.6		16	50	

	15		24.2		24	49	
	16	12.2	21.2	0	32	49	
	17	2.9	13.1	0.7	39	50	
	18	4.8	4.2	0.1	40	52	
	19	9.8	2.0	0.6	41	55	9.82
	20	0.2	0.9		35	57	
	21		0.1		31	59	
	22	1.1	0.1	0.1	29	62	
	23	0.1	4.5	7	27	69	
	24	0	0.9	2.2	27	79	11.5
17/10	1	0.6	0.3	3.2	27	90	11.8
	2	0.5	0.1	2.2	33	100	
	3	0.6	3.0	10.7	41	108	
	4		1.6	4.2	49	113	15.5
	5		0.3	1.8	53	117	
	6	1.4		1.2	53	119	
	7	0	4.9	0.1	53	121	32.1
	8		11.3	6.1	53	121	
	9		0.2	1.9	53	121	
	10		0.5	0.1	55	121	53.2
	11		0.1	2.4	57	121	214
	12		1.0	1.9	59	121	186
	13		1.5	6.8	65	122	193
	14		1.3	5.4	68	126	323
	15		1.0	7.3	70	130	159
	16		0.6	3.3	75	134	117
	17			1.7	83	137	142
	18		0.8	3.6	98	141	132
	19		1.2	1.2	105	144	110
	20		0.7	6.5	106	147	114
	21		0.7	0.3	104	148	107
	22			17.5	101	148	130
	23		0.3	14.4	99	148	245
	24		0.9	5.1	97	146	264
18/10	1		0.2	2.1	97	145	241
	2		0.5	2.3	99	144	212
	3		0.7	4.7	103	143	186
	4		1.8	1.3	110	143	161
	5		0.9	3.6	117	143	144
	6		1.8	6.9	122	142	126
	7	0	13.2	4.1	125	142	112
	8	0	12.5	2.9	125	142	106
	9		6.3	1.6	125	142	103
	10	0	3.8	2.5	121	142	102
	11	2.8	3.0	1.1	118	142	94.9
	12	0.2	0.7		115	145	89.9
	13		0.3		113	149	85.9
	14		0.1	5.4	109	156	83.9
	15		0.4	7.1	108	162	81.9

	16		0.8	1.3	108	168	78.9	
	17		0.4	0.6	108	173	84.9	
	18	0	0.4	3.2	108	175	87.9	
	19	0.1	0.5	3.6	108	176	81.9	
	20	0.1	0.6	2.9	106	175	78.9	
	21		0.1	4.6	104	172	75.9	
	22	0.4		8	101	170	74.0	
	23	5.3		8.6	100	167	72.0	
	24	7.5	0.4	6.1	99	164	71.1	
19/10	1	5.0	1.9	5.4	97	161	75.9	
	2	0.7	2.3	3.6	99	158	81.9	
	3	1.1	2.3	3.8	103	156	108	
	4	7.2	2.2	4.9	107	153	137	
	5	10.1	1.1	8.3	110	152	120	
	6	5.7	1.4	9.6	112	150	107	
	7	10.6	1.4	11.7	118	150	94.9	
	8	13.3	3.3	14.1	123	151	106	
	9	30.6	4.0	16.8	130	155	126	
	10	19.8	4.8	18	138	159	146	
	11	21.2	3.2	13.9	145	167	175	
	12	18.6	1.9	10.0	157	175	177	
	13	18	0.6	9.9	167	183	162	
	14	10.5	0.5	9.9	180	191	151	
	15	12.1	0.5	5.8	192	200	143	
	16	6.3	2.9	6.1	200	208	135	
	17	5.5	1.0	9.3	206	216	124	
	18	10.4	2.9	21	207	222	114	
	19	21.8	17.0	19.4	210	230	130	
	20	14.3	9.0	19.6	212	236	148	
	21	13.3	7.7	29.7	213	240	160	
	22	7.7	12.0	18.8	215	244	200	
	23	5.9	5.3	5.9	219	248	233	
	24	0.4	0.2	2.4	225	254	241	
20/10	1	0	0	0.2	234	265	172	
	2	0	0.1		240	277		
	3				244	286	133	
	4				245	290		
	5	0.1		0.2	242	291	115	
	6				229	288		
	7	0			219	284	104	
	8	0			207	278		
	9				198	273	97.0	
	10				191	267		
	11				183	261	89.9	
	12				176	256		
	13				170	251	87.9	
	14				163	246		
	15				156	241	84.9	
	16				152	237		

	17				147	233	81.9
	18		0.2		142	229	
	19	0	0.2		139	225	77.9
	20	0	0.3		136	222	
	21	0.2	0		133	218	75.0
	22	0.1	0.1		130	215	
	23	0	0.1		126	211	73.0
	24		0		123	208	
21/10	1				118	205	70.1
	2	0			115	201	
	3	0			112	198	
	4				109	195	67.2
	5				106	192	
	6				104	189	
	7		0.2		101	185	64.4
	8		0		100	183	
	9				99	180	
	10				98	178	62.5
	11				97	175	
	12				95	173	
	13				93	170	59.6
	14				90	167	
	15				88	165	
	16				87	163	56.9
	17		0.2		83	160	
	18		0.3		81	158	
	19				81	155	55.0
	20		0.1		81	153	
	21		0.1		81	151	
	22		0		81	149	53.2
	23				81	147	
	24				79	145	
22/10	1	0			74	143	48.7
	2	0.9			71	141	
	3	0.8			68	139	
	4	1.8		0.1	64	137	
	5	0.4		0.5	63	135	
	6	0.1	0.3	0.8	62	133	
	7	0.5	0	2.2	61	130	47.0
	8	0.7	0.2	3.2	63	129	
	9	1.3		4.4	65	127	
	10	0.7		4.5	66	126	
	11	0.1	1.9	2.3	68	125	
	12	0	0.5	0.7	69	123	
	13	0	0.5	0	67	122	47.0
	14	5.1	0.8	0.7	66	123	
	15	2.8	2.1	1	65	124	
	16	0	1.1	0.5	63	123	
	17		0.3		62	122	

	18		0		61	122	
	19		0.4		62	122	46.2
	20	0.2			66	122	
	21	0.2	0.2	0.4	70	123	
	22	0.1	0.7	0.1	75	125	
	23	0.1	0.4	0.1	78	127	
	24	0.5	0.3	0.6	78	128	
23/10	1	0	1.1	0.4	75	130	44.4
	2	0		3.3	71	130	
	3	0.1		1.2	65	131	
	4	0.2	0.7	1.4	61	131	
	5	0	0.5	1.4	57	132	
	6		0	0.2	56	132	
	7		1.6	0.3	55	132	41.9
	8		1.3		57	132	
	9		0.1	1	60	132	
	10	0	1.5	1.3	65	131	
	11		0.6	1.2	69	131	
	12		0.1	5.3	70	130	
	13		1.6	10.2	70	130	43.6
	14		0.1	10.1	68	129	
	15		1.6	2.5	66	128	
	16		0.9	4.7	64	126	
	17		4.4	7.3	61	125	
	18	0.3	4.1	6.2	59	124	
	19	3.9	21.6	9.9	61	122	54.1
	20		15.7	16.9	65	122	
	21		34.2	13.9	75	121	
	22	0	59.9	6.8	83	121	
	23	0.1	52.5	14.8	93	121	
	24	1.6	47.4	8.8	105	122	
24/10	1	9.2	49.4	19.7	131	124	30.6
	2	5.6	74.4	11.9	161	137	
	3	4.7	16.5	4.7	200	168	
	4	8.9	4.2	2.8	246	223	
	5	4.9	4.7	2.6	278	333	
	6	1.3	0.4	2.2	282	416	
	7	2.7	0.5	4.3	272	435	29.1
	8	1.4	4.8	0.4	257	434	
	9	0.8	1.6	0.3	241	425	
	10	6	2.7	5.9	230	412	
	11	15.3	4.3	5.7	227	401	
	12	0.1	0.9	1.5	223	398	
	13	8.3	0	5.8	219	402	27.6
	14	21.8	3.8	17.6	216	404	
	15	20.9	2.8	2.8	211	403	
	16	1.8	0.2	2.3	204	393	
	17	0.2	1.0	2.1	197	381	
	18	0.5	0.9	3.1	191	370	

	19	2	1.4	4.8	187	360	26.9	
	20	2.0	2.0	3.3	185	354		
	21	0.8	0.2	0.1	182	348		
	22	0.3	0.2	0	180	340		
	23	5.6		1.3	178	334		
	24	0.1			175	327		
25/10	1				173	322		
	2			0.1	170	316		
	3		0.4	0.2	166	311		
	4	1	0.6	1.4	162	306		
	5	0.7	0.6	1	155	301		
	6	0.3	0.5	0.2	148	296		
	7	0	0		143	291		
	8	0	0.1		138	287		
	9				134	283		
	10				130	279		
	11				127	275		
	12				125	272		
	13				123	268		
	14				120	265		
	15				115	262		
	16		9.9		114	258		
	17		3.0		111	255		
	18		1.6	1.6	109	252		
	19		4.6		105	248		
	20		4.4		101	245		
	21		6.4	0.1	101	242		
	22		0.1		101	240		
	23		0.1		101	238		
	24		0.3		103	239		
26/10	1			0.1	105	245		
	2		0.2		105	252		
	3		0		101	255		
	4				98	255		
	5				95	252		
	6	0			91	248		
	7				87	242		
	8				82	238		
	9				81	233		
	10	2.3		0	80	229		
	11	2.1		2	82	226		
	12	1.7	3.1	4.6	84	224		
	13	0	23.9	2.2	86	221		
	14		0.1		88	218		
	15				88	216		
	16		1.2		85	214		
	17		5.4		81	212		
	18		6.3		79	210		
	19		22.0		77	210		
	20		0		75	211		
	21				74	213		

	22				76	217
	23	4.3		1.8	79	221
	24			2.6	81	224
27/10	1	8.6			87	225
	2	2	0.2	0.2	91	226
	3	11.6	0.7	0.6	91	227
	4	1.2	0	1.4	90	225
	5	0	0.7	0.1	88	222
	6	2.6		0.1	85	219
	7	5.4			83	215
	8	0.2			80	212
	9	0.4			79	209
	10				78	206
	11			0.2	78	203
	12				79	200
	13				81	198
	14				82	195
	15		0.1		82	193
	16				80	191
	17				78	189
	18				74	186
	19		0.3		70	184
	20		0		68	182
	21				64	180
	22				61	177
	23				63	175
	24				65	173
28/10	1		0.1		68	171
	2		1.1		72	170
	3		0.6		74	168
	4				71	167
	5		0.1		70	165
	6		0.3		69	164
	7	0		0.1	66	162
	8	0			59	160
	9				56	159
	10				53	157
	11	0			53	155
	12	1.5		0.2	53	154
	13	0.8			55	152
	14	0		0.1	59	150
	15	3.6		1.7	62	149
	16	0.7			62	148
	17	2.2			61	147
	18	1.3	0.2	0	59	146
	19	5.8	0.2	0.1	56	144
	20	2.6	0.2	0.4	54	143
	21	19.6	1.2	0.5	52	142
	22	3.4	3.2	4.5	51	143
	23	1.9	10.8	8.2	57	147
	24	0.1	4.8	1.6	63	150

29/10	1	2.3	1.5	0.5	67	154
	2	0.8	0.9	0.3	70	157
	3	0.2		0.6	75	160
	4			3.2	75	163
	5			0.4	75	167
	6	0		0.2	74	171
	7	13			73	175
	8	8.9	0.4		72	178
	9	4.3	1.3	0.2	71	181
	10	1.5	0.7		68	183
	11	0.1	2.7		66	184
	12	0.4	2.2		64	185
	13	0.2	0.8		64	186
	14	0.1	0.1		65	187
	15	0.2	0.4	0.3	67	188
	16	0.1	0.1	0.9	69	189
	17			0.1	69	191
	18				67	192
	19	1.6		3	65	194
	20	5.9	0.1	8.4	61	194
	21	2.1	0.1	0.2	58	194
	22	1	0.1	0.1	56	193
	23	3.1	0.1		55	191
	24	0.2			56	189
30/10	1	0.3			57	188
	2	1.2			59	186
	3	2.8			61	184
	4	1.1			63	182
	5	0.2			65	180
	6		0.1		65	178
	7		0.1		64	176
	8		0.2		62	174
	9		0.1		58	172
	10				56	171
	11				55	169
	12		4.2		51	167
	13		5.7		49	165
	14		0.1	0.5	51	164
	15		1.1	0.1	53	162
	16		0.3		56	160
	17				59	159
	18				59	157
	19				59	156
	20				57	155
	21				53	154
	22				49	154
	23				47	152
	24				47	151
31/10	1				48	150
	2				49	149
	3				50	148

	4				51	147	
	5				53	145	
	6				55	144	
	7		0		53	142	
	8				51	141	
	9				50	140	
	10				49	138	
	11				45	137	
	12				41	135	
	13				41	134	
	14				41	132	
	15				43	130	
	16				49	129	
	17				55	128	
	18				57	127	
	19		0		58	125	
	20				55	124	
	21				52	123	
	22				49	122	
	23				46	120	
	24				42	119	
1/11	1				39	117	30.6
	2				40	116	
	3				41	114	
	4				43	113	
	5			1.2	45	113	
	6	20.9		1.8	47	112	
	7	2.7	2.0	5.5	48	111	29.1
	8	0	8.6	8.4	49	111	
	9		4.8	2.2	49	112	
	10		37.6	6.4	49	113	
	11	0.1	14.5	30.6	49	114	
	12	2.2	16	29.2	49	115	
	13	3.4	36.5	12.3	49	116	27.6
	14	15.4	33.5	16.5	52	120	
	15	8	25.5	12.8	66	126	
	16	7.6	33.0	11.0	127	142	
	17	10.6	18.0	3.8	179	206	
	18	14.5	3.7	6.5	218	314	
	19	4.8	10.5	25.6	237	392	26.9
	20	20.5	20.8	31.9	244	422	
	21	7.8	41.0	14.1	247	430	
	22	4.3	57.5	12.4	254	430	
	23	6.7	56.5	29.7	284	432	
	24	15.7	75.5	12.5	345	441	
2/11	1	4.7	74.7	8.3	387	456	26.9
	2	6.1	59.8	44.1	411	468	
	3	8.1	45.0	9.5	426	473	
	4	10.6	70.0	19.8	434	478	
	5	23.9	57.0	5.1	448	482	

	6	31.2	25.5	39.4	465	487	
	7	57.6	19.0	9.4	486	489	26.9
	8	58.6	20.0	6.4	519	492	
	9	96.7	24.5	17.7	538	496	
	10	65.4	36	25.9	551	500	
	11	76.7	22.5	11.3	567	510	
	12	120.1	3.2	5.8	570	512	52.3
	13	107.2	5.2	25.0	574	514	103
	14	65.7	4.3	5.5	581	517	94.9
	15	27.1	1.5	23.3	576	518	93.9
	16	37.5	5.3	20.7	566	518	112
	17	24.5	10.5	7.3	561	517	119
	18	24.6	8.5	10.2	556	513	125
	19	19.6	19.0	4.8	546	512	132
	20	25.7	7	15.3	541	510	162
	21	34.4	17.5	12.1	536	508	264
	22	39.8	16	19.9	532	505	303
	23	27.2	19.7	22.5	526	502	517
	24	55.6	21.8	18.3	521	500	424
3/11	1	65.4	28	28.5	519	498	416
	2	76.3	34.5	27.7	517	497	398
	3	87.2	48.5	49.8	516	497	382
	4	65.6	30.5	61.7	526	498	367
	5	98.1	5.3	36.5	531	501	357
	6	65.4	4.7	12.4	531	507	365
	7	37.7	4.5	8.7	531	509	426
	8	11.4	6.6	7	531	510	461
	9	8.9	7.4	14.5	528	510	539
	10	19.4	9.5	9.9	527	508	616
	11	33.4	9.5	17.5	524	504	685
	12	19.5	15.0	16.3	518	503	344
	13	15.4	8.0	10.6	511	501	317
	14	20.4	11.5	17	503	499	308
	15	27.7	6.5	11.6	496	496	305
	16	29.4	9.5	14.8	494	493	371
	17	26.9	10.0	15.3	489	492	298
	18	29.2	13.5	19.9	487	491	283
	19	34.5	15.2	8	484	491	274
	20	24.2	7.9	5	481	493	266
	21	27.4	7.1	7.9	480	492	259
	22	5.7	6.2	2.5	474	491	276
	23	5.6	0.6	1.9	466	490	346
	24	3.7	3.1	4.3	457	489	416
4/11	1	23.1	4.9	5.9	451	487	378
	2	18	8.5	21.8	444	486	404
	3	5.5	23	9	438	484	486
	4	19.6	36.5	4.7	434	483	645
	5	18.2	8.9	0.2	434	483	583
	6	32.2	2.4	4.6	432	484	380

	7	2.9	1.2	1.6	426	484	348
	8	19.5	3.0	8.5	420	484	323
	9	5.8	9.0	0.8	416	484	296
	10	11.6	8.0	10.0	407	483	308
	11	4.2	4.5	26.5	399	482	319
	12	7.8	6.0	42.6	388	480	319
	13	7.2	19.5	57.6	381	478	310
	14	7.2	26	37.3	376	476	308
	15	6	29	39.2	383	475	341
	16	8.7	55	3.5	392	473	341
	17	2.6	42.5	29.9	414	472	333
	18	0.1	40	26.4	431	471	352
	19	0.1	16.4	40.8	442	471	376
	20	0.3	18.6	51.4	445	473	361
	21	0.1	25	34.6	444	474	291
	22	1.9	17.5	14.6	442	476	278
	23	1.6	17	1.2	442	478	259
	24	0.9	30	4.6	442	478	248
5/11	1	0.6	31.7	26.5	443	477	222
	2	0.2	16.3	46.3	445	477	212
	3	1.8	13	8.2	446	476	215
	4	0.1	14.5	1.2	444	476	257
	5	5.2	9.0	14.8	441	476	227
	6	2.1	18.5	30.8	436	475	209
	7	1.5	26	46.6	434	475	196
	8	1.4	28.4	22.2	430	475	187
	9	0.2	20.7	48.2	425	474	184
	10		13.3	15.6	424	473	184
	11		6.4	6.7	424	472	203
	12	0	14.1	12.7	424	472	229
	13	0.5	5.4	9.4	424	471	274
	14	1.1	16.6	2.6	421	471	295
	15	1	7.1	1.8	416	471	305
	16	1.2	9.9	4.9	413	470	356
	17	0.8	5.7	3.2	408	469	314
	18	0.2	12.3	1	402	468	305
	19	0.1	4.7	4.3	391	466	245
	20	0	7.4	3.8	377	463	245
	21	0.1	11.6	5.3	368	460	235
	22	1.8	9.5	18.3	355	458	276
	23	3.3	24	18.8	343	456	233
	24	0.6	20.6	15.7	338	454	194
6/11	1	12.8	5.6	6.3	337	452	179
	2	22.5	1.7	10.4	343	454	186
	3	9.1	4.1	14.3	358	456	233
	4	9.1	7.0	0.8	373	457	317
	5	5.6	3.2	0.4	389	456	321
	6	0.3	10.1	0.2	399	456	324
	7	0.1	2.1	0	397	456	328

	8	0	0.1		391	455	291	
	9	0			381	453	276	
	10				372	451	314	
	11				360	448	341	
	12				341	444	341	
	13				328	441	363	
	14				317	437	281	
	15			0.2	305	432	240	
	16				295	428	194	
	17		0.3		285	423	180	
	18	0	1.7		274	419	179	
	19	0.3	0.4		267	415	184	
	20	0.1	0.1	2	257	410	179	
	21	0.2		1.5	252	404	177	
	22	0.4	0.2		245	399	175	
	23	0.3	0.3	0.1	240	395	186	
	24	0.1			234	392	276	
7/11	1	0.1	0.1	2.6	230	389	396	
	2	1.4	0.3	2	225	385	442	
	3	1.5	0.7	2	218	381	328	
	4	0.5	1.8	0.7	215	377	261	
	5	0		1.1	210	373	227	
	6	0		0.3	205	369	198	
	7	0.2		0.2	200	365	176	
	8	0			196	362	159	
	9			0.2	193	359	155	
	10				190	355	152	
	11				187	351	148	
	12				184	348	144	
	13	0	0		181	344	141	
	14	0	0		177	340	137	
	15				173	336	133	
	16	0			170	332	131	
	17	0			166	329	129	
	18	0		0.1	162	325	127	
	19			0.2	159	322	125	
	20			0.3	156	318	124	
	21		0.1		154	315	123	
	22			0.6	151	312	121	
	23		0.2	0.5	149	309	119	
	24		0.2	0.7	148	306	119	
8/11	1		0.1	0.2	147	303	118	
	2	0	0.4	0.6	144	300		
	3	0.1	0.3		142	298		
	4	0.1	0.3	0.3	137	295	114	
	5		0	0.3	133	292		
	6		0.4	0.2	129	289		
	7		0.2	0	126	286	110	
	8		0		123	284		

	9		0.2	121	282		
	10		0.3	119	279	104	
	11		0	118	277		
	12			118	274		
	13			117	272	99.0	
	14			115	269		
	15	0		113	267		
	16	0.1		111	264	94.9	
	17	0.2	0.1	109	262		
	18	0.5	0.3	107	259		
	19	0.5	0.3	104	257	91.9	
	20	0.1	0	103	255		
	21	0	0.2	102	252		
	22		0.2	101	250	89.9	
	23		0.1	100	248		
	24		0.1	99	246		
9/11	1		0	97	244	86.9	
	2		0.1	96	241		
	3		0.1	95	239		
	4			94	237		
	5			92	235		
	6			91	232		
	7			90	230	79.9	
	8			85	228		
	9			81	226		
	10			80	224		
	11			79	222		
	12			83	220		
	13			85	218	73.0	
	14			85	216		
	15			85	214		
	16			83	212		
	17			80	210		
	18			78	208		
	19	0		77	205	71.1	
	20	0	0.9	76	203		
	21		0.7	74	201		
	22		1.3	73	199		
	23		0.6	73	197		
	24			74	195		
10/11	1			75	194	67.2	
	2			74	192		
	3		0.2	73	190		
	4			71	188		
	5			70	186		
	6			69	185		
	7			67	182	64.4	
	8			63	180		
	9			61	178		

	10			59	176		
	11			61	175		
	12			64	173		
	13			68	171	60.6	
	14			71	170		
	15			72	168		
	16			70	166		
	17			67	165		
	18			64	163		
	19			60	161	57.8	
	20			57	159		
	21			56	158		
	22	0.2		55	156		
	23	0		55	154		
	24	0.1		57	153		
11/11	1			61	152	55.0	
	2			65	150		
	3			67	149		
	4			67	148		
	5			63	147		
	6		0	59	146		
	7	0		57	144	52.3	
	8			56	143		
	9			53	142		
	10			48	140		
	11			50	139		
	12			51	138		
	13			56	137	50.5	
	14			61	136		
	15			63	136		
	16			59	135		
	17			57	134		
	18			54	133		
	19	0		51	132	48.7	
	20			45	131		
	21			43	130		
	22			41	128		
	23			41	127		
	24			43	126		
12/11	1			45	125	47.0	
	2			49	125		
	3			51	124		
	4			53	124		
	5			49	123		
	6			45	122		
	7	0		43	121	45.3	
	8			40	120		
	9			37	120		
	10			33	118		

	11			33	118		
	12			35	117		
	13			39	116	43.6	
	14			41	116		
	15			44	115		
	16			47	115		
	17			45	114		
	18			43	114		
	19			39	112	41.9	
	20			35	112		
	21			31	111		
	22			29	110		
	23			29	109		
	24			29	108		
13/11	1			31	108	41.0	
	2			33	107		
	3			35	107		
	4			37	106		
	5			35	106		
	6		0	33	105		
	7	0		31	105	40.2	
	8			29	105		
	9			28	104		
	10			25	104		
	11			24	103		
	12			26	102		
	13		0.7	28	102	38.5	
	14		0.6	33	101		
	15	0.6		36	101		
	16			42	101		
	17			42	101		
	18			38	101		
	19	0.2		35	100	36.9	
	20	0.2		32	100		
	21			29	99		
	22			27	99		
	23			25	98		
	24			29	99		
14/11	1	0.2		31	99	35.3	
	2	0.1		33	99		
	3			35	100		
	4			36	100		
	5			37	100		
	6			35	100		
	7			34	99	34.5	
	8			32	99		
	9			29	98		
	10		0	27	97		
	11		0.2	25	96		

	12				27	95		
	13		0.5		29	95	33.7	
	14			3.0	31	94		
	15		2.0		33	94		
	16		9.4		39	94		
	17		0.2		45	94		
	18				43	94		
	19	0.2	3.3		39	94	36.1	
	20		0.2		35	94		
	21		0.7		31	93		
	22				29	93		
	23				27	92		
	24				29	92		
15/11	1				31	93	33.7	
	2				32	93		
	3			0	35	94		
	4				37	94		
	5			0.1	39	94		
	6	0.3		3.0	37	94		
	7	11.3		1.6	36	94	32.1	
	8	4.5	2.2	0.2	35	94		
	9		1.5	0	33	94		
	10		0.1		30	94		
	11	0.2			28	93		
	12	0	0.4	0	28	92		
	13		0.1	0.3	28	92	32.1	
	14			2.7	30	91		
	15			2.2	32	91		
	16		0.2	0.2	39	91		
	17		1.5	0.1	46	92		
	18		0.2	0.5	45	92		
	19		1.1	0.4	43	93	31.4	
	20		0.1	0.2	41	93		
	21		0.1		37	93		
	22		0.2	0.2	35	93		
	23			0.5	31	92		
	24		0.1		31	92		

7.2.2. Temperature

Date	**Temperature (°C)**		
	Hue	*Nam Dang*	*Aluoi*
15/10	25.3	25.1	22.0
16	25.2	24.3	21.6
17	25.7	23.9	21.2
18	25.0	22.2	19.4
19	21.1	20.6	18.4
20	24.9	25.0	21.5
21	23.9	23.6	20.7
22	24.0	23.7	21.5
23	25.9	24.3	21.8
24	24.8	24.2	21.7
25	25.8	25.5	23.0
26	25.5	24.7	22.4
27	25.4	25.2	22.1
28	24.8	24.5	21.9
29	24.5	25.0	21.9
30	25.7	25.5	22.7
31	26.8	26.9	23.8
1/11	25.2	23.0	21.1
2	22.3	22.0	19.8
3	20.5	20.3	18.4
4	22.8	21.5	20.0
5	25.0	23.3	21.4
6	24.7	25.4	22.4
7	23.1	22.7	20.7
8	23.4	22.8	21.2
9	24.8	24.4	21.9
10	25.7	25.1	22.6
11	25.9	25.6	23.7
12	26.2	25.8	23.6
13	25.9	25.2	23.0
14	25.5	24.7	21.9
15	24.1	22.8	19.9

7.2.3. TRMM files from DAAC

Item ID	Date
2A12.991014.10818.5.HDF	10-15
2A12.991016.10839.5.HDF	10-16
2A12.991016.10849.5.HDF	10-17
2A12.991017.10854.5.HDF	10-17
2A12.991018.10880.5.HDF	10-19
2A12.991019.10885.5.HDF	10-19
2A12.991019.10895.5.HDF	10-20
2A12.991021.10916.5.HDF	10-21
2A12.991021.10926.5.HDF	10-22
2A12.991023.10947.5.HDF	10-23
2A12.991023.10957.5.HDF	10-23
2A12.991024.10962.5.HDF	10-24
2A12.991025.10988.5.HDF	10-25
2A12.991026.10993.5.HDF	10-26
2A12.991028.11024.5.HDF	10-28
2A12.991028.11034.5.HDF	10-28
2A12.991029.11055.5.HDF	10-30
2A12.991030.11065.5.HDF	10-30
2A12.991101.11096.5.HDF	11-01
2A12.991101.11101.5.HDF	11-02
2A12.991103.11127.5.HDF	11-03
2A12.991103.11132.5.HDF	11-04
2A12.991104.11142.5.HDF	11-04
2A12.991105.11163.5.HDF	11-06
2A12.991106.11173.5.HDF	11-06
2A12.991107.11194.5.HDF	11-08
2A12.991108.11204.5.HDF	11-08
2A12.991108.11209.5.HDF	11-09
2A12.991110.11235.5.HDF	11-10
2A12.991110.11240.5.HDF	11-11
2A12.991112.11266.5.HDF	11-12
2A12.991113.11281.5.HDF	11-13
2A12.991114.11302.5.HDF	11-14
2A12.991115.11312.5.HDF	11-15

7.3. Appendix 3: TRMM Images Pprcessing

7.3.1. Orbit Viewer software

The Orbit Viewer is a tool for displaying the standard data products of TRMM. Since 1997, the TRMM Science Data and Information System (TSDIS) has developed and distributed the Orbit Viewer. The Orbit Viewer runs under several varieties of UNIX, including Linux, and under Microsoft Windows 2000. The Orbit Viewer can be downloaded at no cost from the TSDIS web site http://tsdis.gsfc.nasa.gov. From this web site, can also be downloaded the most recent version of the tutorials.

7.3.2. Creating a grid subset

Once an array has been displayed in the zoom image of the Orbit Viewer's main window, the data can be saved from that image to a data subset. The steps that must be followed depend on whether the array is a swath or grid. This section describes how to save grids and how to convert a swath into a grid and save it as a grid. The next section describes how to save swaths without converting them first into grids. The grids in TRMM standard products and in subsets created by the Orbit Viewer contain bins that are equally spaced in latitude and longitude. To create a data subset, select the File Save_Data menu item. In response, a Save Data window will appear (Figure 25).

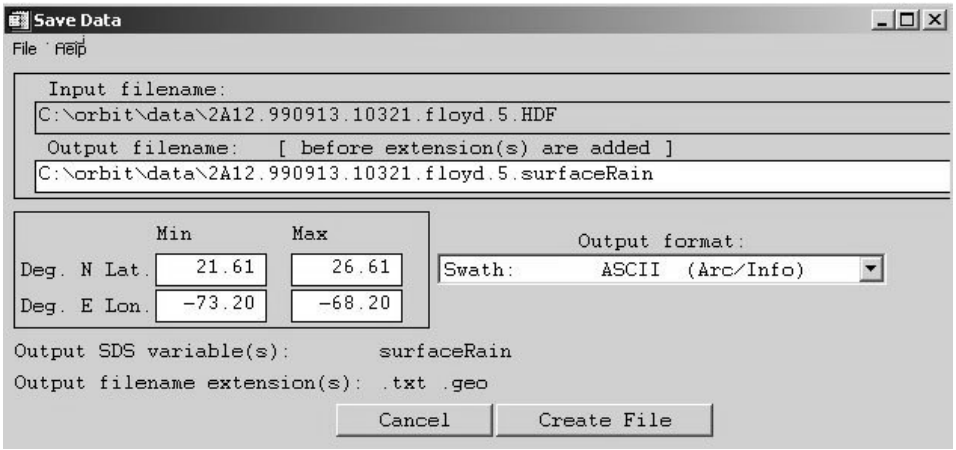

Figure 25. Save data window in Orbit Viewer

At the top of the Save Data window is listed the filename of the currently displayed file and the filename for the data subset that will be created. On the left side is listed the latitude and longitude limits of the data to be written. If the currently displayed array is a grid, the lat/long limits will be fixed so that the whole grid is written. If the currently displayed array is a swath, then the user will be able to edit the limits to determine how much of the swath is written to the subset. On the right is a pull-down menu that determines the format of the subset. When the user finishes adjusting the settings of the Save Data window, the Create File button may be clicked.

If a swath array is displayed, but the user wants to save it as a latitude/longitude grid, the Orbit Viewer could perform that conversion before writing the subset. To do that, the pull-down menu in the Save Data window must be used to choose a format in the "swath grid" category. To change the resolution of the grid that will be computed, the File Swath_to_Grid_Options menu item can be selected. The process of creating a grid reduces the resolution of the data, and therefore, the resulting grid should only be used for an initial examination of the data.

The Orbit Viewer can save grids in any of the following formats: HDF, ASCII text, GrADS binary, and Arc/Info text. In all of the grid subsets, the outer limits of the grid in latitude and longitude are written as well as the actual grid data. In the case of Arc/info (Environmental Systems Research Institute ESRI), the Orbit Viewer can only save data in the text version of the Arc/Info format. Once the subset is created, it can be read into Arc/Info and converted to the native GIS binary format that is compatible with other GIS packages such as Arc/View and ILWIS.

There are actually two kinds of Arc/Info text formats, one for grid data and one for swath data. Below is a very small example of an Arc/Info grid file created by the Orbit Viewer from the 2A25.nearSurfRain swath array. Since this is a swath array, the Orbit Viewer converts it to a grid before writing it into the Arc/Info file. The metadata that defines the size and geographic limits of the grid appear at the top of the file. The "ncol" field is the number of columns, "nrow" is the number of rows, "xllcorner" is the lower-left edge of the grid in degrees of east longitude, "yllcorner" is the lower left edge of the grid in degrees of north latitude, "cellsize" is the size of each grid cell in degrees. Each row of the grid is written as a line in the ASCII file, starting with the northernmost row.

Arc/Info Grid Text File
ncol 5
nrow 5
xllcorner –82.72
yllcorner 14.00
cellsize 4.0

0.000	0.000	-99.000	-99.000	-99.000
0.009	0.023	0.091	0.128	-99.000
0.002	0.051	4.293	3.492	0.003
-99.000	0.025	1.911	0.321	1.566
-99.000	-99.000	-99.000	-99.000	0.445

7.3.3. Creating a swath subset

Swath data is a little more complicated than grid data. A grid is defined by just a rectangular data array and the geographic limits of the grid. A swath is defined by a data array (with "txt" file extension) plus an array that contains the latitude and longitude of each observation (with "geo" extension). In TRMM files, the latitude and longitude values are stored in an array called "geolocation".

To create HDF or ASCII text subsets of swath data, the File Save_Data menu item must be selected from the Orbit Viewer's main window. Arc/Info text subsets of swath arrays can be created, and these

subsets are called “point files.” Below is a truncated example of the data file (left) and the geolocation file (right) for Arc/Info.

Data file (*.txt)		Geolocation file (*.geo)		
1,	5.5	1,	-70.0,	25.0
2,	5.0	2,	-70.0,	30.0
3,	23.2	3,	-65.0,	30.0
. . .			. . .	
END				

This type of output format was selected because it is easily imported in ILWIS as table format. The geolocation files that had lat-long coordinates had to be changed to UTM Northing and Easting respectively (UTM 48N zone). One table for each TRMM file was created and point maps were obtained through the Table Operation command. The point maps were used to interpolate the data and raster images were in this way obtained.